Design of the cold and thermal neutron moderators for the European Spallation Source

Zanini, L.; Andersen, K. H.; Batkov, K.; Klinkby, E. B.; Mezei, F.; Schönfeldt, T.; Takibayev, A.

Published in:
Nuclear Inst. and Methods in Physics Research, A

Link to article, DOI:
10.1016/j.nima.2019.01.003

Publication date:
2019

Document Version
Peer reviewed version

Accepted Manuscript

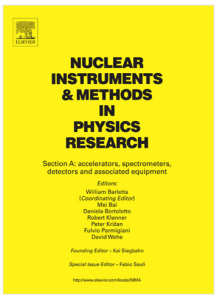

Design of the cold and thermal neutron moderators for the European Spallation Source

L. Zanini, K.H. Andersen, K. Batkov, F. Mezei, A. Takibayev, E.B. Klinkby, T. Schönfeldt

PII: S0168-9002(19)30008-7
DOI: https://doi.org/10.1016/j.nima.2019.01.003
Reference: NIMA 61776

To appear in: *Nuclear Inst. and Methods in Physics Research, A*

Received date : 14 August 2018
Accepted date : 2 January 2019

Please cite this article as: L. Zanini, K.H. Andersen, K. Batkov et al., Design of the cold and thermal neutron moderators for the European Spallation Source, *Nuclear Inst. and Methods in Physics Research, A* (2019), https://doi.org/10.1016/j.nima.2019.01.003

Available online at www.sciencedirect.com
ScienceDirect
Journal Logo
Nuclear Instruments and Methods in Physics Research, Section A 0 (2018) 1–65

Design of the cold and thermal neutron moderators for the European Spallation Source

L. Zanini, K. H. Andersen, K. Batkov, F. Mezei, A. Takibayev

European Spallation Source ESS ERIC, PO Box 176, 22100 Lund, Sweden

E. B. Klinkby, T. Schönfeldt

DTU Nutech, Technical University of Denmark, DTU Risø Campus, Frederiksborgvej 399, DK-4000 Roskilde, Denmark

Abstract

At the European Spallation Source (ESS), neutrons will be generated by spallation induced by a 2-GeV proton beam on a tungsten target. ESS will have a grid of 42 beamports available for a variety of neutron scattering experiments. Neutron moderators will provide thermal and cold neutrons to the instruments, allowing bispectral beam extraction wherever needed.

The moderators were designed by adopting a holistic design approach that has considered brightness, brightness transfer and beam extraction constraints, resulting in a system with the following main features: low-dimensional moderators for enhanced brightness and maximum flux to the sample; a single moderator system placed above the spallation target; lateral shape of the moderators optimized for bispectral extraction. A moderator with a vertical extraction surface of 3 cm was chosen as the result of the optimization process.

With all initial instruments pointing to the top moderator, and a beamport system that allows the possibility to extract neutrons from above and below the target, the adopted configuration opens the possibility to have different types of moderators below the target, so that other neutron beams of different intensity, or spectral shape, with respect to the ones delivered by the top moderator, could be envisaged, adding additional scientific opportunities to the facility without having the need to build a second target station.

Keywords: low-dimensional moderators, source brightness, parahydrogen, water, neutron beam extraction, long pulse sources

1. Introduction

The European Spallation Source (ESS), presently in construction in Lund, Sweden, aims at starting the user program in 2023 [1]. At 5 MW time-average power, and 125 MW peak power, ESS will be the most powerful neutron source in the world for neutron scattering studies of condensed matter. Neutrons will be produced by a 2 GeV proton beam impinging on a target made of tungsten. ESS will be the first high-power accelerator driven long pulse source [2], the pulse length of the beam will be of 2.86 ms, with 14 Hz repetition rate.

Neutron moderators, placed next to the spallation target and designed to slow down neutrons from MeV to the sub-eV range, are a key component of the neutron source. While the accelerator power is a key parameter to indicate the performance of the facility, the brightness of the neutron source, for cold and thermal neutrons, is more relevant for the neutron scattering experiments, because it is a quantity directly related to the number of neutrons at the sample.

The first complete moderator design was presented in the Technical Design Report (TDR) [1] and in Ref. [3]. The TDR cold moderators were pure parahydrogen cylindrical moderators of 16 cm diameter and 13 cm height, and their calculated brightness exceeded the design goal of ESS, to deliver a cold peak brightness a factor of 30 higher than the official ILL cold brightness [4]. After the work for the TDR, the ESS neutronic team led a research effort aimed at designing moderators with further increased brightness. The design of the moderators was redefined based on the concept of low-dimensional moderators [5, 6]. As low-dimensional moderators represent a new idea for enhanced moderator brightness, we discuss in detail their physics properties in Section 2.

In this discussion we concentrate on *flat*, quasi-two-dimensional moderators, because it is the design basis for the ESS moderators. (quasi-one dimensional moderators are discussed in AppendixB). In Section 3 the different moderator concepts that were considered for ESS are discussed. In Section 4 the beam extraction aspects and their role on the moderator design are discussed. The performances of the moderators are compared in Section 5. In Section 6 the *butterfly*-shape moderator, the selected moderator shape, is described and characterized in detail. Conclusions and some initial suggestions for future upgrade possibilities are given in Section 7. The method of brightness calculation, and the tube moderators (one of the options for future upgrades at ESS) are discussed in the appendices.

All calculations have been performed with MCNPX 2.7.0 [7–9] using the default Bertini/Dresner spallation/evaporation models and ENDF/B-VII nuclear data libraries.

2. Properties of low-dimensional moderators

Low-dimensional moderators have been proposed in recent years to increase the brightness of neutron sources. Studies on moderators of reduced dimensions were carried out from first principles to conceptual design for two high-power spallation sources under design: ESS [5, 6, 10] and the SNS second target station [11]. In these facilities a large number of beam lines covering beam extraction sectors 60°-wide or more is foreseen. For this purpose, two-dimensional moderators are considered. Following the more radical concept of quasi-one-dimensional moderators [6], ideas to use *tube* moderators in reactors [6] and compact sources [12] have been brought up, exploiting the strong brightness and directionality of such moderators, which gives an extra advantage in specific situations where the moderator is feeding only a few beam lines covering a narrow angular span of about 10-20°. While possible future applications of tube moderators for

Figure 1. Basic physics model of a pancake moderator. *Left*: horizontal cut. *Right*: vertical cut of the target-moderator-reflector configuration. The 2-GeV proton beam is hitting the target perpendicular to the plane of the figure.

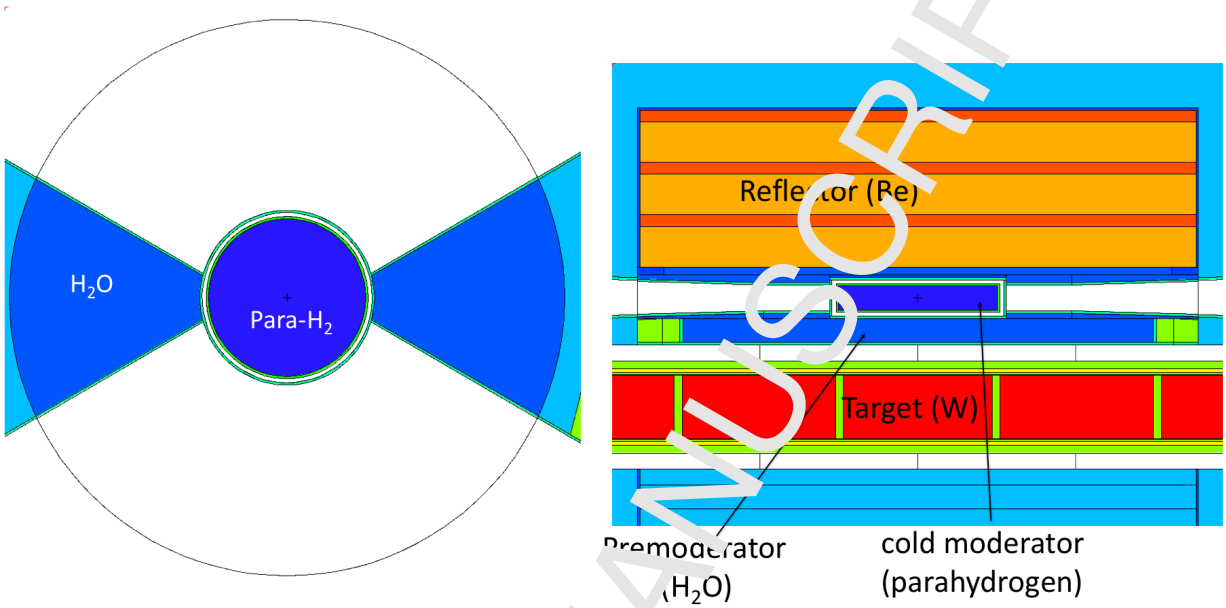

ESS are discussed in the appendix, in this section we examine the properties of two-dimensional moderators, which are the basis for the ESS design.

2.1. Quantification of the brightness gain

The fundamental properties of the low-dimensional moderators can be understood by the study of a simple quasi-two-dimensional moderator of cylindrical shape, which we called *pancake*: a cylindrical aluminum vessel filled with pure para-hydrogen, placed above a spallation target, with a beryllium reflector on top, and a water premoderator between target and moderator (Figure 1). The premoderator shapes the energy spectrum of the neutrons, which, coming from the spallation target, have high energies in the range of 1-2 MeV. We consider the case of neutron beam extraction over a large angular range, with two sectors covering 120° each because this applies directly to ESS (a wider opening area is in practice not possible for a configuration where the proton beam hits the target horizontally). However, the discussion can be generalized to different beam extraction configurations.

We define the brightness B in AppendixA. Although the brightness is time-dependent, we describe it in terms of a peak and a time-average brightness, since it is largely constant during the duration of the proton pulse (apart from the rise and fall-off tails). For the peak brightness, we assume that B is equal to the plateau value reached during a 2.86 ms long pulse. For the time-average brightness, the pulse structure of

Figure 2. Cold peak brightness wavelength spectra for moderators of different height, calculated from the geometry of Figure 1. Neutrons are extracted in an exit direction perpendicular to the incoming proton beam, at the center of the 120° sector of Figure 1 (left).

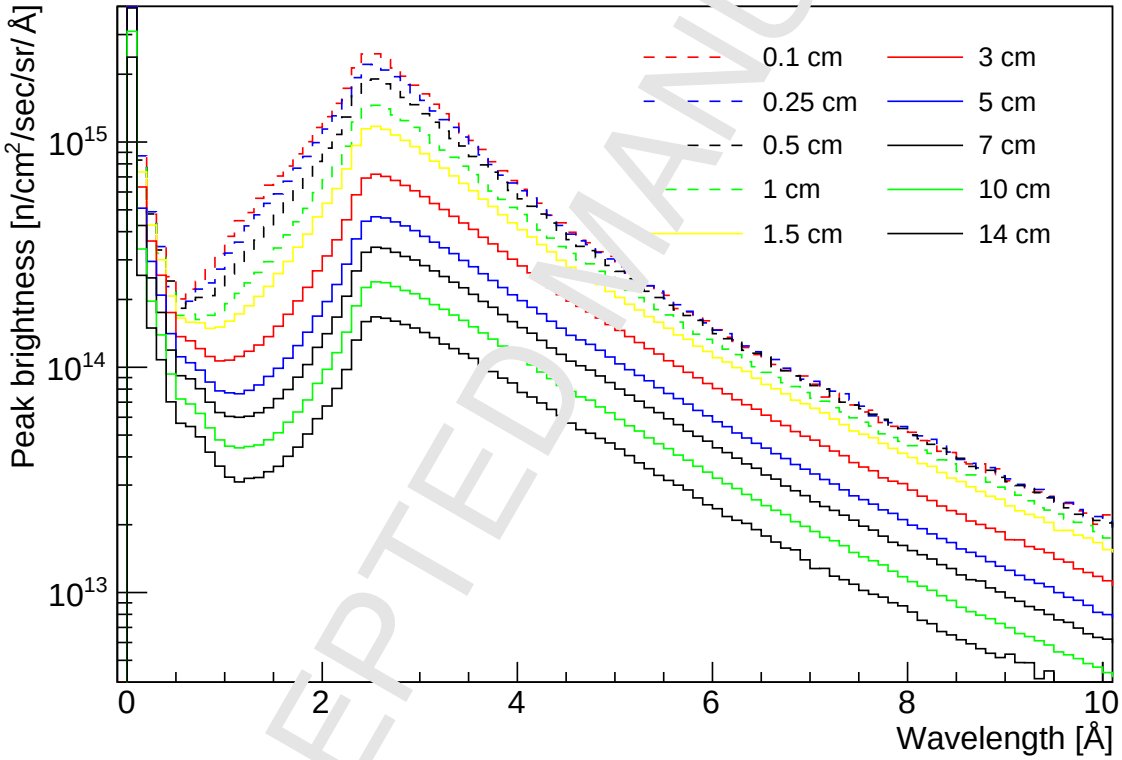

Figure 3. Same as Figure 2, for thermal neutrons, extracted from wider wings.

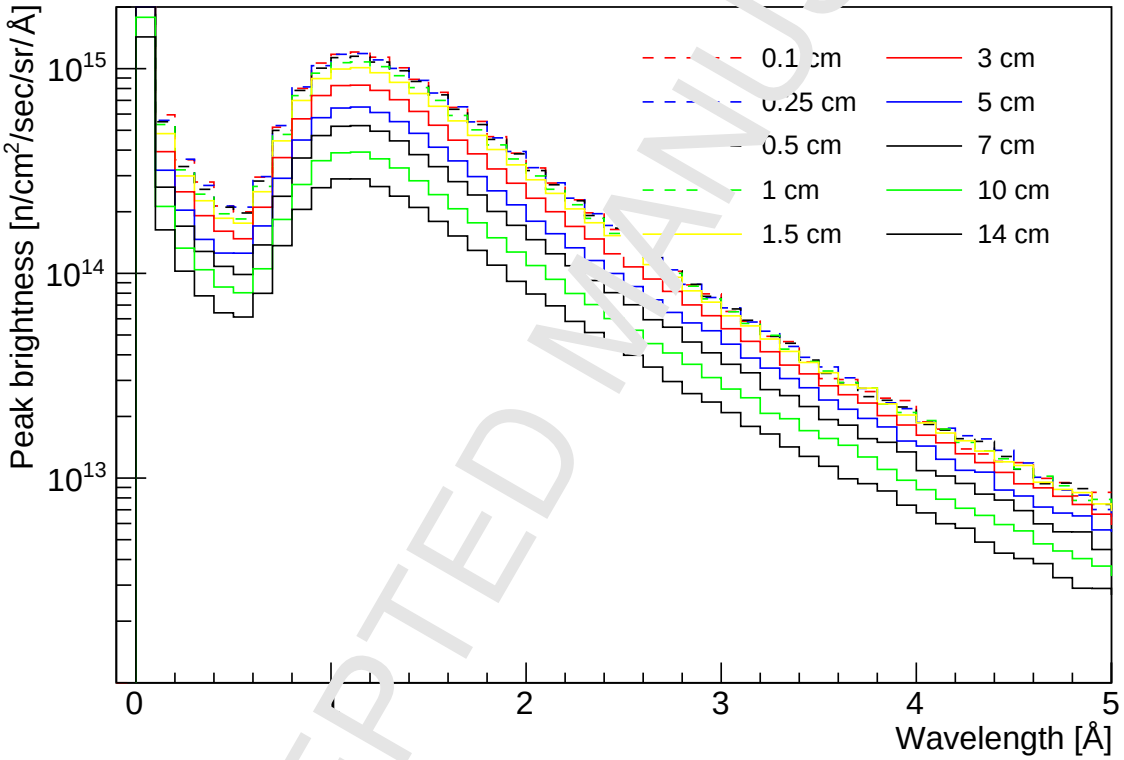

Figure 4. Cold brightness gains with respect to 10 cm tall moderator, from the spectra shown in Figure 2.

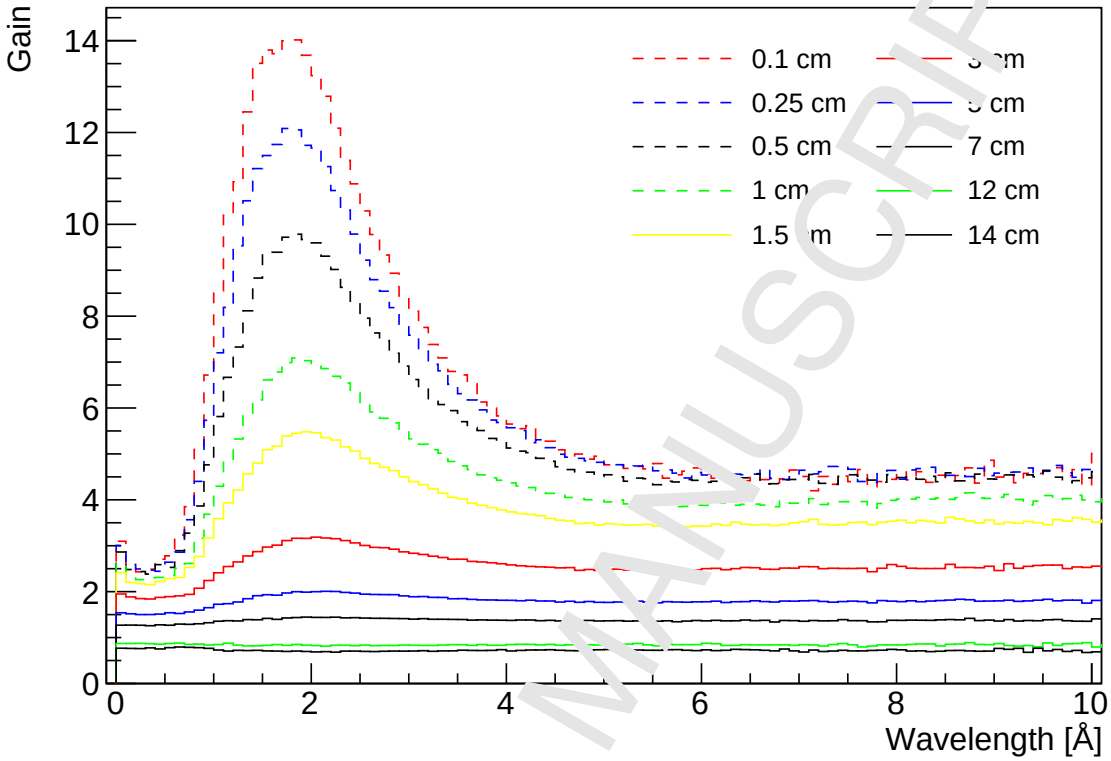

the beam is not considered and the ratio between peak and time-average brightness is T/τ=25, where the repetition period $T = 1/14$ Hz and the pulse length $\tau \approx 2.86$ ms.

In Figure 2 and Figure 3 the spectral brightness from the cold and thermal parts of the moderators are shown, respectively. Cold neutrons are extracted from the center of the cold moderator, from an area of fixed width of 6 cm, with height equal to the height of the moderator. The brightness is averaged over the extraction surface. In the case of the thermal moderator, neutrons are extracted from a window of the same area, from the water moderator placed at the side of the cold moderator of Figure 1.

The wavelength spectra, divided by the brightness of the 10-cm-tall moderator, thus representing the brightness gain as a function of the wavelength relative to the 10 cm moderator, are shown in Figures 4 and 5. There is a qualitative difference between the gain from the thermal moderators and parahydrogen, as a function of the wavelength: while for thermal neutrons the gain does not vary much within the wavelength span shown in Figure 5, a strong variation is observed for cold neutrons.

For the determination of the optimal height of the moderator, and in general for its neutronic design, we considered integrated cold and thermal brightness in different energy ranges of interest for most common

Figure 5. Same as Figure 4, for thermal neutro

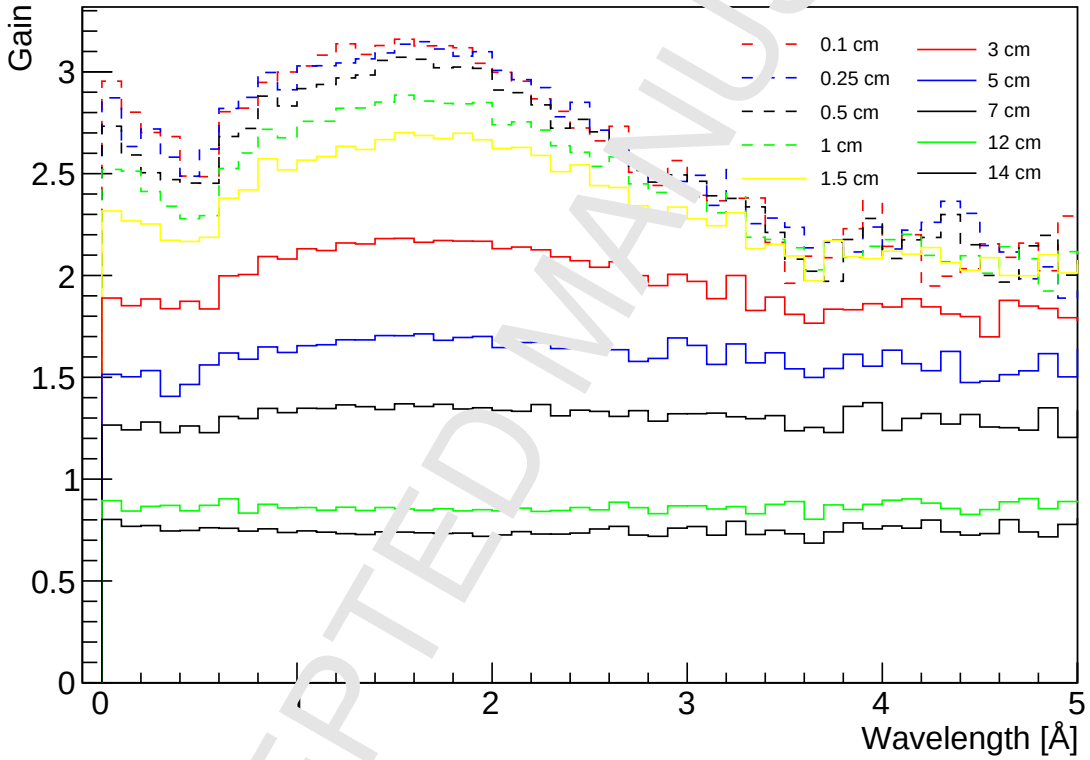

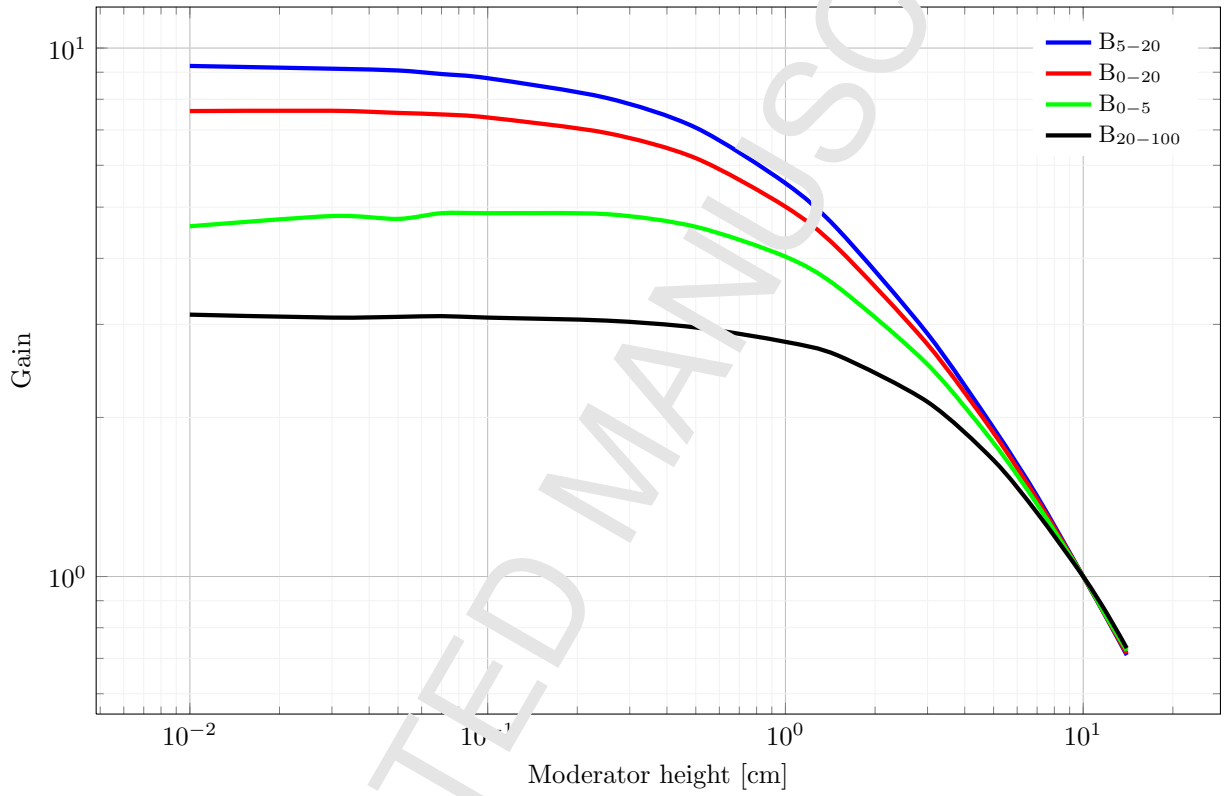

Figure 6. Cold and thermal integrated brightness as a function of moderator height, calculated from the geometry of Figure 1. Neutrons are extracted in an exit direction perpendicular to the incoming proton beam, at the center of the 120° sector of Figure 1. The brightness is calculated for a 6-cm wide horizontal width, the vertical range being equal to the parahydrogen height. Integral brightnesses are relative to the brightnesses for the 10 cm high moderator.

applications in neutron scattering (see AppendixA): for cold neutrons, B_{0-5} below 5 meV (4 Å), B_{5-20} between 5 meV and 20 meV (2 Å), averaged over the cold moderator surface. For thermal neutrons, B_{20-100}, between 20 meV and 100 meV (0.9 Å), averaged over the thermal moderator surface, was used.

Figure 6 shows the relative gain in thermal and cold brightness as a function of the moderator height, for integrated brightness in different energy ranges. We observe for all (thermal and cold) integrated brightnesses a general increase by reducing the moderator height.

We argue in the following that the gains observed are in part due to general properties of hydrogenous moderators, related to the mean free path of thermal neutrons in such materials. The additional gain in parahydrogen with respect to water can be attributed to the properties of its total neutron cross section. The gain is particularly strong for the cold moderator in the wavelength region between about 1 Å and 3 Å (Figure 4).

B_{5-20} reaches a constant value for moderator height approaching zero. For colder neutrons, B_{0-5} slightly decreases after reaching a maximum for about 2 mm height.

The total cross section in parahydrogen for neutrons in the thermal region is about σ=20-30 barn, which translates to a mean free path (MFP) in parahydrogen of about 1 cm. For water, the MFP of thermal neutrons is about 0.3 cm. For the moderator height d much lower than the MFP, the number of collisions, including those leading to neutrons exiting the moderator, is proportional to σd; as the brightness is averaged over the emission surface with area $A = Wd$ (the product of width W and height d), one can expect that for small moderator thicknesses B is independent of d. This explains the near constant value of B observed in Figure 6 for low moderator heights.

We consider in the following subsections different contributions to the observed gains. We discuss first the role of the reflector.

2.2. Reflector response

The reflector surrounding the moderator has the function to return neutrons that have not gone through the moderator, or that have escaped from it, to the moderator itself, giving them another chance to be moderated and redirected towards the beam extraction channels. For long pulses the time response of the reflector (of the order of 100 µs) is of no concern. Beryllium is the material of choice for reflectors in pulsed neutrons sources. The removal of beryllium around the moderator to extract thermal and cold neutrons has the effect of reducing the brightness with respect to the maximum theoretical *unperturbed* brightness, i.e., the configuration where the moderator is fully surrounded by reflector material.

The amount of reflector material removed increases with the height of the moderator, if neutrons are extracted from the entire moderator surface. However, it also varies in the horizontal plane (where instruments are placed), depending on the beam extraction configuration and in particular on the number of beamlines that point to the moderator.

We therefore consider separately these two aspects: the effect of the removal of reflector material for moderators of different height, and the effect of removal of reflector material in the horizontal plane of beam extraction.

In Ref. [5] we examined the unperturbed brightness. Comparing the unperturbed brightness of 10 cm and 3 cm tall moderators, it was found that the 3 cm tall moderator is 1.6 times brighter than the 10 cm tall moderator, for neutrons below 5 meV. It was also found that for a 10-cm tall moderator, the unperturbed brightness is a factor 1.7 higher than the *perturbed* brightness, calculated for a configuration with two 60° beam extraction openings in the reflector.

On the other hand, from Figure 6 the cold perturbed brightness difference between two moderators with height of 10 cm and 3 cm is of a factor 2.5, which is close to the product of the two gain factors. Thus it appears that the overal brightness increase effect is due to two main factors, of roughly equal amount; one due to removal of reflector material, the other, observed in the comparison of the unperturbed configuration, due to other physics effects. It is however not possible to fully disentangle the two effects: in the unperturbed configuration, by reducing the height of the moderator the amount of beryllium is also increased; therefore the brightness increase in the unperturbed configuration is due in part to increase of reflector, in part to additional physics effects discussed below.

Besides the effect of the reflector on the different heights of the moderator, there is an effect also on the angular size of the opening for beam extraction. Instruments at ESS will be arranged around the moderators covering four angular sectors of 60°, which will be paired forming two large angular sectors of 120°, one consisting of the North and West sectors, the other one of the South and East sectors (see Figure 7).

In order to further study the effect of the reflector removal, we considered two geometries (Figure 8), with different openings in the reflector, which were both considered for ESS: a configuration with two large opening configuration of 120°, with 21 beamports per opening, and a configuration of two openings of 60°, with 11 beamports per opening.

Figure 9 shows the brightness distributions for individual beamports. As a result of the reflector removal, going from 60° to 120° results in an average brightness loss of 6% for the 3 cm moderator, while it is twice as much for the 10 cm moderator. The effect is larger for a taller moderator, because of the larger amount of beryllium removed.

In the original design of the TDR two identical volume moderators (placed above and below the target) viewed two face-to-face openings of 60° [1], so that half of the beamports of one 120° sector would point to the top moderator, the other half to the bottom. This had the advantage that each moderator would have two openings of 60°, and not of 120°, thus increasing the amount of reflector surrounding the moderator. It had however the disadvantage that two different moderators had to be operated, as the use of a single moderator for the whole instrument suite would have resulted in a too big loss of brightness. Such loss would be lower in the case of low-dimensional moderators.

A goal of ESS is to provide a beamport grid covering an angle of 240°. In practice the choice, by using low-dimensional moderators, is between a single flat moderator with two 120° openings, or two identical flat moderators, placed above and below the spallation target, with two 60° openings each. As shown in Figure 9, the difference in brightness is of about 6 %. This is calculated considering a flat moderator above the target, and a steel reflector at the bottom. In reality, if a flat moderator with two 60° openings is placed at the top, another moderator must be placed at the bottom. Cross-talk effects between top and bottom moderator exist (see Section 2.8), according to which the brightness of a moderator is reduced, if another moderator is placed below the target, by at least 5 %. Therefore, a single low-dimensional moderator with two 120° openings will have in a real situation about the same performance as two low-dimensional moderators with two 60° openings each. The performance of the single moderator can be further increased if a fast neutron reflector on the other side of the target is designed to increase its performance (see Section 2.8), which is not possible if there are two moderators.

In summary, we see that the effects related to the reflector play two roles, both in advantage of low-dimensional moderators: first, the brightness increase effect by reducing the moderator height; second, the possibility to use a single moderator, which would not have been acceptable for tall moderators, because of the stronger brightness decrease.

The latter finding had a profound influence on the design of the ESS facility, as it was understood at an early stage that only one low-dimensional moderator was needed. By following this path, options on the use of a second moderator from the start of ESS were investigated. After the realization that all of the ESS initial instruments would perform well by pointing at the top moderator, as discussed in [13], the decision was that only one moderator would be installed at the start of ESS, thus adding a wide array of possibilities for future upgrades using the place below the target. Such an approach also reduces costs and risks of malfunction.

2.3. Physics effects

2.3.1. Parahydrogen

Liquid parahydrogen is the chosen material for cold neutron production at ESS, and is used in other facilities including J-PARC. The advantage of using pure parahydrogen, as opposed to a mixture of ortho- and parahydrogen, stems from the peculiarity of its total neutron cross section [14, 15]: below about 80 meV the total cross section starts decreasing, from a value of about 30 barn, until reaching about 1 barn below 15 meV. The reason for this drop is due to the spin-dependence of the neutron-proton interaction, and to the spin-dependent interference between the neutron wave functions scattered from the two protons in the hydrogen molecule [16]. At 20 K, 99.8 % of hydrogen is in parahydrogen form at thermal equilibrium [17]. As the main reaction for neutrons in the meV energy range is the para- to orthohydrogen spin-flip transition, which requires 14.7 meV, this reaction is not possible below this energy, explaining the drop in the cross

section. The inelastic cross section for para- to orthohydrogen, in the range between 14.7 meV to about 70 meV, increases from about 1 barn to about 30 barn, which is comparable to the elastic scattering in orthohydrogen at the same energy. The density of liquid hydrogen and the behavior of its cross section are responsible for several effects relevant to moderator neutronics, namely: the thermalization of the neutrons in about 1 cm from the moderator walls; the near-transparency to cold neutrons; the non-complete thermalization of the neutron spectrum.

The neutron spectrum entering the moderator has a strong thermal component, due to the presence of the premoderator on one side (between target and moderator), and of the beryllium reflector, which returns partially moderated neutrons to the moderator, on the other side. Figure 10 shows the energy spectra calculated in regions above and below the moderator, namely the water premoderator, and a cooling water layer placed in the bottom part of the reflector. Neutrons from the reflector side are mostly thermalized.

In Figure 4 a peak in gain factor is observed for neutrons in the wavelength range between about 1 Å and 3 Å, corresponding to an energy range between about 9 meV and 80 meV. These neutrons are not fully thermalized in the moderator, and most of them have probably only one collision before exiting the moderator. Because of the small MFP, such neutrons are concentrated on the edges of the moderator, on both target and reflector sides. Due to the sudden drop of the total neutron cross section in parahydrogen below 70 meV, the MFP of cold neutrons increases to about 10 cm: the medium becomes *quasi*-transparent to cold neutrons which therefore have low probability to be scattered.

This effect in most evident in Figure 11, which shows the vertical distribution of the brightness for neutrons in the wavelength range between 1.5 Å and 2.2 Å (i.e., corresponding to B_{17-36}, where the gain observed in Figure 4 is maximum), for moderators of 1.5 cm, 3 cm and 10 cm height. The two peaks get closer to each other for flatter moderators. The fact that, for this energy range, the brightness is enhanced at the edges of the moderator, explains the large gain seen in Figure 6: for the 10 cm tall moderator, the brightness in the central part of the moderator is strongly reduced, leading to a surface-average brightness decrease. The concentration of neutrons towards the edges of the moderators is also evident in the brightness distribution maps of B_{0-20} shown in Figure 12 for moderators of height of 1.5 cm, 3 cm and 10 cm. These maps are pinhole images of the brightness distribution on the moderator surface. For the 10-cm tall moderator there are two areas in the moderator of increased brightness, one on the bottom side of the moderator (the target side), one on the top part (the reflector side). A similar figure was calculated for the coupled parahydrogen volume moderator at J-PARC [18]. This non-uniform brightness distribution has been experimentally confirmed by a brightness map measurement of the J-PARC coupled moderator [19]. Our calculations show that the effect is much less pronounced for the 3 cm moderator, and almost cancelled for the 1.5 cm one. This feature is apparent also from Figure 13 and Figure 14 in which the brightness B_{0-20} and B_{0-5} projection across the moderator height, as a function of the vertical position, for three pancake geometries of 1.5 cm, 3 cm and 10 cm height, is shown. The increase of the brightness at the moderator edges is less pronounced for

colder neutrons. We interpret this result as due to the fact that to slow down neutrons from thermal to cold energies below 5 meV on average requires more than one collision, which would extend the volume of the production region of neutrons of this energy.

2.3.2. Water

The brightness increase is observed also for the water moderator, although less pronounced than for parahydrogen: it is of about a factor of 2 (Figure 6), from a 10 cm moderator to a 3 cm moderator.

We can expect the reflector effect to be similar for water and parahydrogen. The MFP of thermal neutrons in water is 3 mm, which contributes to an increase in brightness for low dimensional moderators. However, the edge effects observed for parahydrogen, due to its cross section, cannot be observed in water, and therefore the overal gain is lower. Figure 15 shows the distribution of B_{20-100} across the height of the water moderator. As expected, an overall brightness increase is observed, but without edge effects.

2.3.3. Directionality

The moderator and reflector response, combined with the properties of the parahydrogen, result in a directional emission of low-dimensional cold moderators: the moderator-shape induced directionality translates into higher flux in the horizontal direction with a roughly triangular angular dependence and a FWHM of about 40°. See Figure 16, as well as Ref. [6]. The physical reason for the directional emission is related to the properties discussed above; the cold neutron density increases near the interface of a parahydrogen moderator with the reflector within a depth of the order of the mean free path of the thermal neutrons in parahydrogen (about 1 cm). The cold neutron emission from a parahydrogen moderator, in contrast, effectively happens from a volume within the 10-times higher mean free path of cold neutrons measured from the neutron emission window of the moderator. Thus the neutron emission probability is higher in directions where a larger volume of the moderator material is seen.

In contrast and comparison, the angular distribution in the vertical direction of the thermal neutron beam from the water moderator (Figure 17), shows a much lower directionality. The directionality of the water moderator in the vertical direction roughly follows the expected cosine dependence [26], displaying a broad peak falling to zero intensity at 90°.

2.3.4. Neutron absorption

Due to the significant absorption cross-section of thermal neutrons (0.3 barn at 2200 m/s) in hydrogen, a volume moderator tends to function as a parasitic absorber. This absorption term is reduced in a flat moderator, due to the lower content of hydrogenous material. We calculated that about 10% of the neutrons entering a 10 cm tall cylindrical moderator are captured in hydrogen, while about 3% are captured in a 3 cm tall moderator. Therefore the relative gain in using a flatter moderator is at the per cent level. Similar gains are found for water.

2.4. Total neutron emission and heat load

Figure 18 illustrates two additional aspects of low-dimensional moderators, by comparing total neutron emission and heat load in the cold moderator as a function of the moderator height. The total neutron emission or *intensity* is proportional to the product of the brightness and the area of the emission surface of the moderator.

The total intensity approaches a maximum for moderator heights larger than about 3 cm: a 3-cm tall moderator, while it is about 2.5 times brighter than a 10 cm one, delivers roughly 80% of its neutron intensity. The higher brightness almost compensates the smaller emission surface by providing a total number of emitted neutrons almost as high. Above 10 cm height, the total number of neutrons emitted approaches a constant value. The implication of this result is that to increase the intensity of neutron emission one should not increase the height of a parahydrogen moderator. Rather, other types of moderators should be considered, such as large-volume D_2 moderators.

The heat load in the moderator (parahydrogen and aluminum cryogenic parts) increases with the moderator volume (black curve in Figure 18). Thus, flat moderators have an advantage in terms of requirements on the total capacity of the cryogenic systems. It must be said however that there are other challenges in the design of the cooling of cold moderators, related to the peak heat deposition in the system, and to the flow rate of the hydrogen, that must be addressed in the engineering design.

2.5. Premoderator

The premoderator changes the shape of the neutron spectrum from the spallation target, bringing neutron energies down from the MeV to the thermal range. Usually the premoderator is a layer of water between cold moderator and target. Its thickness is determined by a balance of optimal spectral shaping, by the need to minimize the distance target-moderator, and to minimize neutron absorption.

A thickness of 3 cm was found as optimal; concerning the lateral dimensions, we found that a disk-shaped, extended premoderator, with radius practically equal to the Be reflector, gives a substantial gain in both thermal and cold brightness. Figure 19 shows the relative variation of cold and thermal moderator brightness with the radius of a disk-shaped premoderator. In this sensitivity study, the gain is different depending on the material placed outside the premoderator, i.e., in the ring with inner radius equal to the radius of the premoderator, and outer radius equal to the radius of the beryllium reflector. If there is void, there is a steady increase of both thermal and cold brightness, reaching the maximum for a 30 cm radius disk. By placing a reflector material (in this case, beryllium with 30% water cooling), there is a maximum cold brightness for a premoderator of about 15 cm radius. This could be an option for future upgrades. The present configuration has a steel ring with inner radius of 30 cm.

Figure 7. View of the 42 ESS beamport inserts each of 3.5 m length, located in four beam extraction sectors of 60°. The proton beam comes from the right in the figure. The tips of the beamports are at 2 m from the center of the moderator. The beamports are labeled according to the name of the sectors (North, South, East, West). Angular spacing between beamports in the North and East sectors is of 6°. In the West and South sectors alternating angular spacing of 5.7° and 6.3° between the beamports is used.

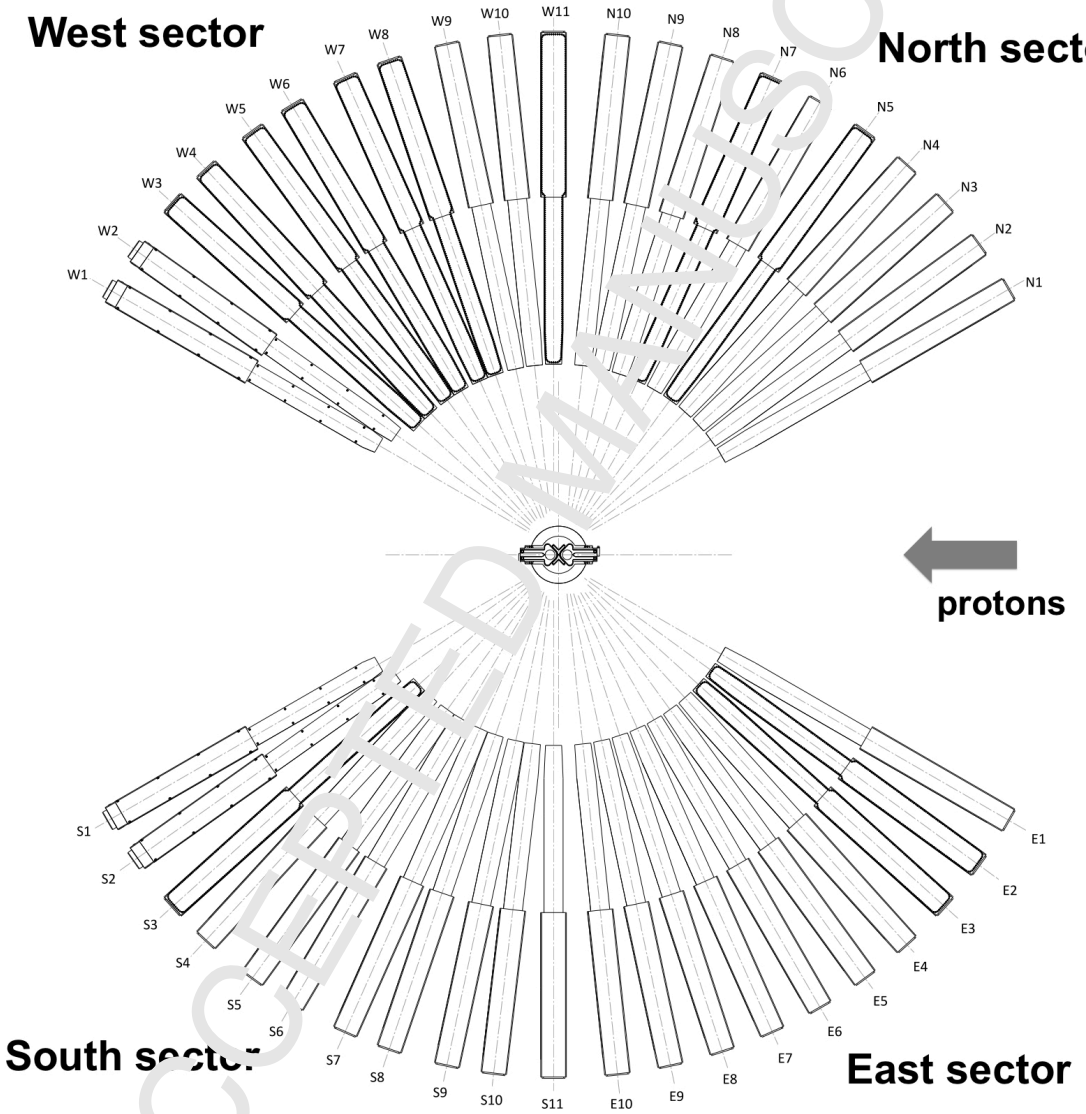

2.6. Orthohydrogen contamination

Figure 20 shows the variation of the cold brightness from a 3-cm tall moderator (in this case of butterfly-2 type, see Section 3.3) as a function of the parahydrogen fraction in the moderator. Maximum performance of low-dimensional moderators requires pure parahydrogen and ideally 100 % parahydrogen should be used. The aim during ESS operation is to achieve a parahydrogen fraction of at least 99.5 % by using catalyzers. Thus small fractions of orthohydrogen are expected, which may slightly affect the neutronic performance of the moderator. In our calculations we assumed 99.5 % parahydrogen, but we had to specify it as 100 % in the model; the reason is because recent experimental results [15] indicate that the ENDF/B-VII measured cross section did not account for an impurity of orthohydrogen of 0.5 % in the hydrogen samples.

In the following two subsections we discuss two properties which are not specific to low-dimensional moderators, but are linked to the design of the moderator systems. The information on the size and location of hotspot of neutron production indirectly dictates the dimension of the moderators, as well as the ideal location of the cold and thermal neutron moderators. The cross-talk between the areas above and below the target is also of interest and can be possibly exploited to increase the moderator brightness.

2.7. Hotspot

Figure 21 shows the map of high-energy ($E > 0.1$ MeV) neutrons from the spallation-evaporation process in the tungsten, assuming 2 GeV protons. The plane of the color map is at the vertical coordinate $Z = 8$ cm, just above the tungsten target and below the water premoderator. To give an idea of the relative dimensions of the moderators and of the neutron hot spot, the geometries of the butterfly (discussed in detail in Section 6) and pancake moderators are superimposed to the neutron flux map, even though the moderators are placed above the plane where this fast neutron map is calculated. The dimensions and lateral positions of both moderators in the figure are optimized for maximum cold brightness across the 120° sectors. This figure confirms that the dimension of the moderators should be comparable to the source of spallation-evaporation neutrons, as expected. This figure also suggests that it is convenient, if possible, to place both thermal and cold sources above the hot spot. This is one of the arguments in favor of the butterfly moderator (see Section 5) and the thermal moderator brightness is higher if the water moderator is placed closer to the center of the hot spot.

2.8. Cross talk between moderators and fast neutron reflectors

The beam extraction system at ESS is designed such that neutrons can be extracted from two angular sectors of 120° each, from above and below the target. The two beam extraction areas above and below the target are not completely independent of each other as neutrons generated or reflected in one region of the target can travel to the other side if their energy is high enough to cross the target wheel. The size of this effect might be increased by the lack of moderating material in the target, which would increase the

absorption of neutrons in the target itself. Thus, the brightness of the moderator placed above the spallation target may depend to some extent on what is placed on the other side.

At ESS this opportunity can be exploited, considering also that ESS is a long pulse facility, and therefore an increase of the width of the time distribution of the neutrons within the long pulse is not of primary concern. If only one moderator system on the top side of the target is present, it is worthwhile considering different options to design a fast neutron reflector placed below the target, to increase the brightness of the top moderator. Such study can be of interest also if two moderator systems are implemented, at least in some cases, for instance if the second moderator system requires a significant neutron and gamma shielding to allow reaching very low temperature (this is the case for some moderators for Ultra Cold Neutrons or Very Cold Neutrons) [20–22]. In that case, the presence of these shields, which are typically heavy metals (such as Bi or Pb) with good properties of fast neutron reflection, could be exploited to increase the brightness of the top moderator.

We considered a few cases using some typical fast neutron reflector materials. Table 1 indicates the gain factors relative to the two-moderator configuration, i.e., a configuration where a moderator/reflector system similar to the top one is placed at the bottom. This is the configuration that results in the lowest brightness, due to the presence of the extended premoderator, as well as the water moderator and coolant, which thermalize the fast neutrons preventing them from crossing the spallation target and reaching the top moderator. On the other hand, if materials that can reflect fast neutrons, such as copper, lead, tungsten, or steel, are used, a significant brightness increase is obtained on the moderators placed at the top. If beryllium is used at the bottom, the brightness increase is not as large as for heavier metals. This is due to the fact that in beryllium neutrons are reflected but also partially slowed down, and a significant part of the neutrons reflected will be absorbed by the tungsten target.

The effect depends on the material used, but also on the amount of water coolant used. The calculations with a tungsten reflector are performed using the same effective density of the tungsten in the spallation target, and assuming helium cooling. It is worth noting that the reflectors absorb a heat load of the order of 500 kW (calculated for steel reflector). Their cooling is therefore quite demanding.

2.9. Background from high-energy neutrons

Neutron scattering research mainly uses slow neutron beams with energies below a few eV. Fast neutrons can preferentially escape the target shielding through the slow neutron beamports. They are also emitted by scattering on the structures around the moderators also viewed by the beam lines. High-energy neutrons can be thermalized by scattering on structures and materials in the experimental halls and ultimately contribute to the background of the slow neutron detectors in the neutron scattering instruments. This is a an issue for all neutron sources; we want to investigate if in the *low-dimensional* moderator concept adopted for ESS the slow neutron signal to fast neutron background emission ratio will be more or less favorable than for

existing spallation sources.

2.9.1. Figure of merit

The figure of merit (FOM) in neutron data collection can be conveniently defined as the square of the signal-to-noise ratio (where by definition both signal and noise are expressed in units of counting time). This corresponds to the data collection rate, i.e. the inverse of the time needed to achieve a given signal-to-noise ratio. The *noise* must be defined as the uncertainty of the measured value of the signal S.

There are two main sources of uncertainties: the statistical precision of the counts measured and the systematic uncertainties and instabilities, which are independent of counting statistics. Considering the issues we are concerned with here, we can restrict the analysis to the statistical precision of the data (assumed to be stable and understood concerning their origin). Other systematic errors are independent of the neutron beam intensities, but of course they become more and more dominant, as the statistical accuracy of the data improves, e.g. by the new level of neutron intensities ESS will offer.

The statistical noise of the signal S will be proportional to $\sqrt{S+B}$, where B is the background. The measured raw neutron counts for both S and B are proportional to the data collection time t, thus the data collection rate is the inverse of the time needed to achieve a given statistical signal-to-noise ratio. The background B has two main components: B_S coming from the slow neutrons delivered to the sample and its environment for the intended observations (usually the main part of B) and B_F due to fast neutrons coming through the beamline or through the shielding of other beamlines, etc. Thus

$$FOM = \frac{S^2}{S + B_S + B_F} \tag{1}$$

In the denominator the first two terms are proportional to the slow neutron beam intensity, the last to the fast neutron production.

Shielding measures that reduce B_F without any effect on S are always useful, to varying degrees. If such a measure impacts both S and B the balance is what matters. For example, if both the slow neutron and the fast neutron production change by the same factor n, the change of FOM will be proportional to n. So the data collection gains of ESS compared to other facilities will be proportional to the delivered neutron beam intensities (i.e. some 10–100 times higher than the other sources) under the assumption that the fast neutron background also increases in the same proportions. If the fast neutron background increases less than proportionally to the slow neutron production rate, the FOM will be for some experiments higher than proportional to the beam intensity gain, primarily in cases where B_F is comparable to or larger than S.

2.9.2. Fast neutron background at ESS.

The total number of fast neutrons emitted is, as for all neutron sources, about the same as that of the moderated neutrons, and it is the beam extraction and shielding equipment that ensures that only a very

small fraction of these neutrons turn up as counts in the detectors (which have in addition low detection efficiencies for fast neutrons).

Figure 22 shows the simulated vertical distribution of the points of emission of neutrons with $E > 1$ eV from the moderator area, for three different pancake moderator heights.

These "emission points" are defined by the backward extrapolation of the neutron trajectories entering the beam line openings to their crossing of the nominal neutron emmiting surface of the cold moderator or to its vertical continuation. In reality, these neutrons are directly generated either by collision with atoms in the volume of the moderating material or by collision with atoms in the structures around the moderator such as the moderator vessel, its insulating housing, the reflector and the coolants.

Since the back trajectory simply follows the direction of the neutron as determined at radius 2 m, the method implicitly assumes that no scattering along the trajectory occurs. for neutrons originating elsewhere than from the moderators, this assumption is not strictly valid, causing a "blur" to the apparent emission point of these neutrons.

The main conclusions from the figure, and considering also Figure 14, can be summarized as follows:

- The total fast neutron emission by flat moderators is less than for the tall one (about 50 % for 1.5 cm moderator height and about 67 % for 3 cm moderator height).

- There is some fast neutron emission outside the moderator window, which amounts to about 36 % of the total fast neutron emission for the 10 cm moderator, 45 % of the total for the 3 cm high moderator, and 51 % of the total for the 1.5 cm high moderator.

- The ratio of the deliverable cold neutron intensity (which scales with the brightness) to the total fast neutron emission is about 3 times more favorable for the 1.5 cm moderator than for the 10 cm one.

Based on the results in Figure 22, Figure 23 shows the relative evolution of the ratio S/B_F of the signal (which is proportional to the cold neutron brightness B_{0-5}, cf. Figure 14) to the emission of > 1 eV fast background neutrons that are coming from the central 8 cm high effective neutron emission area around the middle of the moderator. This means that the assumed background emission conservatively also includes fast neutrons coming from outside the nominal moderator emission surface for moderators of < 8 cm height, while fully excluding these neutrons for taller moderators.

Our MCNPX simulations of detailed models of the ESS target monolith system have shown that the neutron moderators and their immediate vicinity emit towards the beam-line openings in the monolith shielding about as many > 1 eV energy "fast" neutrons (which are assumed to contribute to the background detected at the instruments) as slow neutrons for use in neutron scattering experiments on the instruments (cfr Figure 14 and Figure 22). The emission of fast neutrons geometrically peaks at the edges of the moderators, including areas around and outside the viewed nominal face of the moderator. The ratio of

Figure 8. Pancake geometry, with openings in the reflector of 120° (left), and 60° (right).

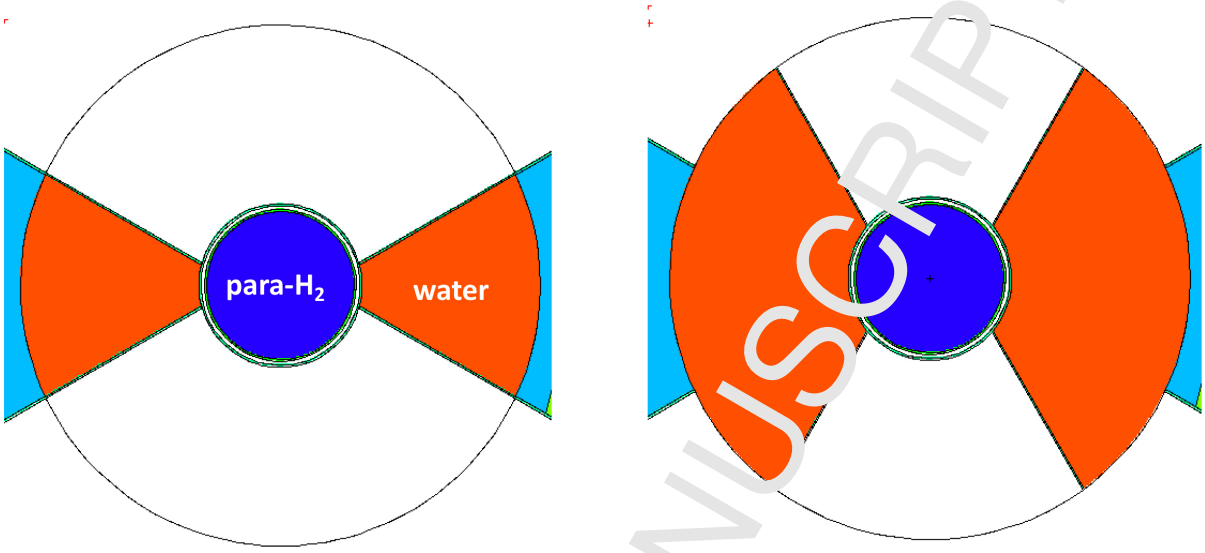

slow to fast neutron emission is significantly more favorable for the low dimensional, flat ESS moderators than for the conventional larger beam cross section moderators at existing spallation sources.

3. Moderator concepts

In this section we describe the moderator concepts that were considered for ESS. We start from the volume-moderator configuration of the TDR, then two low-dimensional moderator concepts which were seriously considered for the facility are described.

3.1. Volume moderator: TDR

The TDR design was based on the J-PARC coupled volume parahydrogen moderator [18]. In the TDR baseline configuration, there are two volume moderators filled with pure parahydrogen. The MCNPX model shown in Figure 24 reproduces the engineering design developed during the target station design update phase [1]. The moderators have a diameter of 16 cm and a height of 13 cm. The moderators are surrounded by light water premoderators (except for the cold neutron extraction window), of which the most important part, from the neutronic point of view, is the layer between target and moderator, which is 2 cm thick. The window surface of the cold moderators for beam extraction is of 12 × 12 cm^2. A variation from the J-PARC design is the presence, on the sides of the cold moderators, of thermal moderators for thermal or bispectral extraction. They consist of 4 cm thick water slabs with a surface area for neutron extraction of 12 × 11

Figure 9. B_{0-20} angular distribution for a 3 cm and 10 cm tall pancakes, with 60° and 120° openings in the reflector allowing for 21 and 11 beamports with 6° separation, respectively. The brightness is averaged over the extraction surface, with fixed width of 6 cm, and height equal to the height of the moderator. Beamport angles are defined with respect to the direction of the proton beam, from left to right in Figure 8.

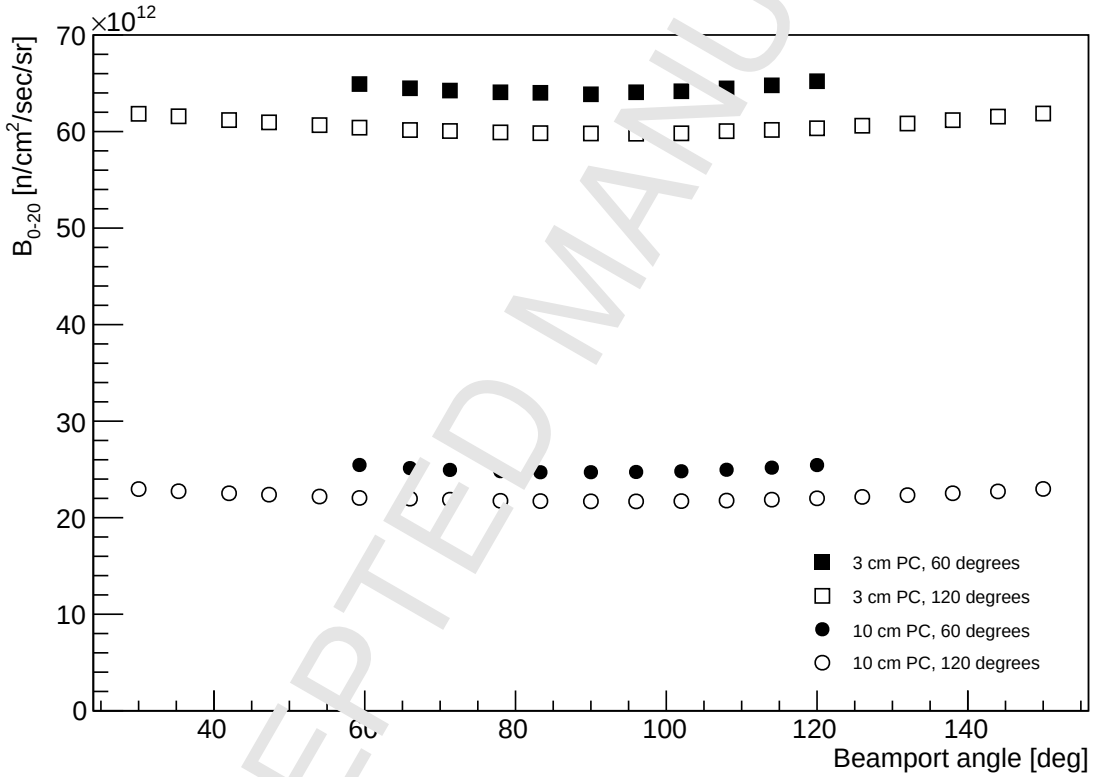

Figure 10. Average flux per unit lethargy inside the cold moderator, the water premoderator, and in the bottom part of the reflector, above the moderator. The flux is calculated using the f4 track-length estimator.

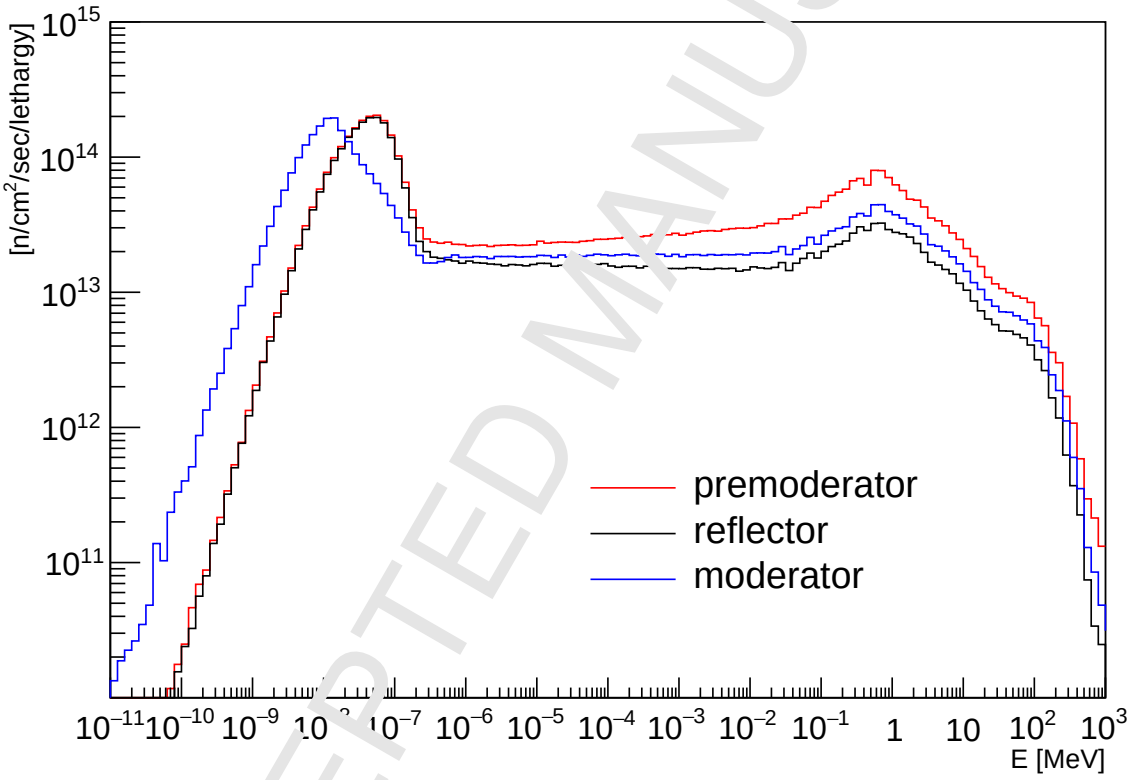

cm^2. The openings in the reflector for beam extraction are of 60°, with two openings per moderator, as shown in the figure. There are two identical thermal-cold moderators, one above and one below the target. The openings in the reflector are arranged so that, of the four 60° sectors, each two 60° sectors, above and below the target, form a 120° sector available for the beamports. More information is available in [1, 3].

3.2. Pancake low-dimensional moderators

The first low-dimensional design considered was the pancake moderator [16], which has been extensively discussed in the previous section, as it forms a convenient basis to determine the properties of low-dimensional moderators. The pancake consists of a disk-shaped (3 cm height, 20 cm diameter) cold moderator (see Figure 1). The basic cylindrical shape comes from the need to serve cold neutron instruments in a 2 × 120° suite. Thermal neutrons are extracted from the sides of the cold moderator which contain water. The need of bispectral extraction implies that a design solution must be found to allow for bispectral extraction. For the pancake, two options are possible, and are discussed in the next section.

3.3. Butterfly low-dimensional moderators

Butterfly-shaped moderators [23–25] consist of a modified version of the pancake, where the thermal source is moved to the center of the moderator. The goal of this design is to adapt to the beam extraction configuration of ESS and provide bright bispectral neutron beams for the whole instrument suite. The first idea behind this concept is to have both thermal and cold sources close to the hot spot of neutron production (see Section 2.7 and Figure 21, left), thus reaching high thermal and cold brightness, and having a design capable of delivering a good bispectral beam over the full 2 × 120° beam extraction sector. Two variants of this design were considered. The first moderator, that will be used at the start of operation, is the so-called *butterfly 2* (Figure 25, bottom). It consists of two distinct cold moderators separated by a thermal cross-shaped moderator and will be operated until the start of the user program. The second variant is the *butterfly 1* (Figure 25, top).

The drivers for the butterfly design were the following:

- place cold and thermal moderators on the hot spot, in order to provide high thermal and cold brightness for a required extraction area of at least 3 (height)×6 (width) cm^2 for both thermal and cold moderators.
- exploit to some extent, also the concept of tube moderators (discussed in [6] and in the appendix), thanks to the geometry of the cold moderator.
- keep a relatively compact shape to ease the beam extraction: for all the 42 beamports, the thermal and cold extraction surfaces lie next to each other, being placed on the two sides of the focal points (see Section 4.4), allowing instruments to see the brightest part of thermal and cold moderators. Such

moderators fit well for a beam extraction in the two 120° sectors; the brightness variation across the sectors is within 15%.

Before comparing the neutronic performance of the different moderator concepts we describe in detail the beam extraction principles and implementation for ESS, to better understand their role in the design of the moderators.

4. Beam extraction

4.1. Design features for instrument performance

For a high-performance instrument suite, the moderator assembly of any facility for neutron beam instruments needs to be designed with three key performance indicators in mind:

1. high source brightness;
2. ability to extract the right amount of phase space for each beamline;
3. ability to install the required number of beamlines.

At ESS, two additional factors were included in the design considerations:

4. ability of each beamline to freely choose between viewing a cold source, a thermal source, or, using a bispectral mirror assembly, a bispectral source;
5. upgradeability.

Achieving high brightness, the first performance indicator, gave the main figure of merit used in the moderator design and is the main focus of the present paper. However, the other performance indicators were also used in the moderator design. In this section key features of the other performance factors are described, and in particular their link to the design of the ESS moderator assembly. All these performance indicators gave practical constraints and guides on the design of the moderator. This is however only one side of the work, as every proposed design implied an extensive study of the brightness transfer to the instruments, which in turn gave additional inputs to the moderator design, in an iterative process. This iterative work, from the point of view of beam extraction and brightness transfer to the instruments, is described in detail in [13].

4.2. Phase space

Most neutron beam instruments use the neutron beam to illuminate a sample of a material to be studied. The huge range of types and geometries of samples reflects the diversity of the science which can be addressed with beams of slow neutrons [1]. The main limiting features to the required phase space of the neutron beam are, however, fairly well-known.

Figure 11. B_{17-36} distribution across the moderator height, for cold neutrons, for three cylidrical moderators with 1.5 cm, 3 cm and 10 cm height, for neutrons between 1.5 Å and 2.2 Å. Moderator edges are marked by dashed vertical lines. The vertical position is relative to the center of the spallation target.

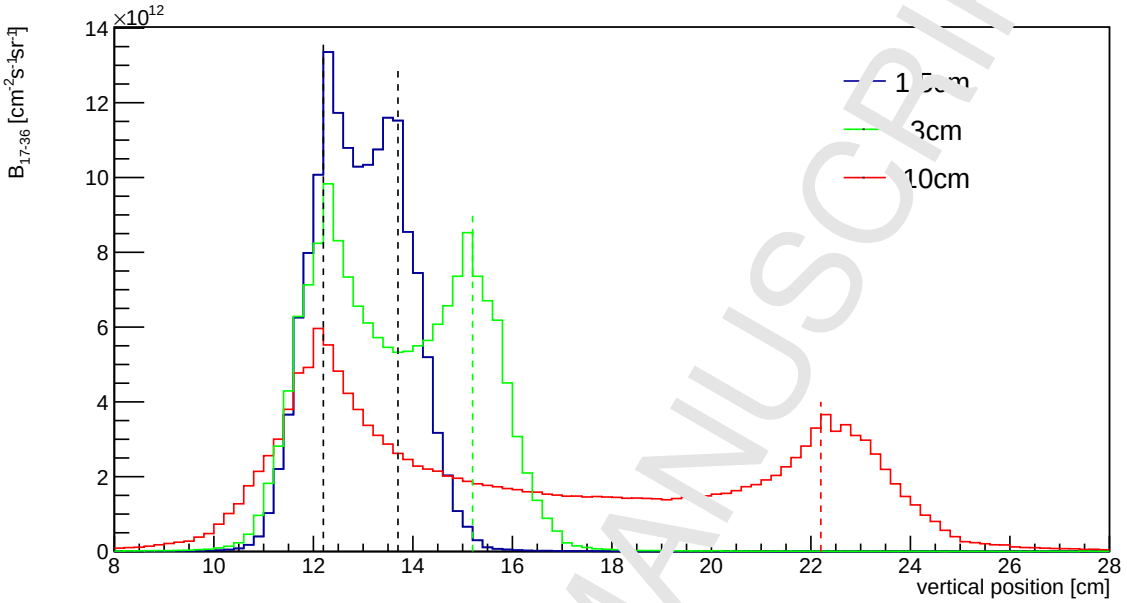

4.2.1. Beam size

The beam size typically needs to be adapted to the sample size. In a few cases, samples can be very large, up to several metres in linear dimension. However, in these cases, the purpose of the neutron beam investigation is always to measure local properties with a spatial resolution which is much smaller than the size of the sample, typically of the order of mm's or less. Most neutron scattering experiments are flux-limited, due to the intrinsically low neutron source brightness compared to, e.g. synchrotron light sources. For optimal experimental conditions, sample volumes for neutron experiments are therefore usually fairly large to compensate for the low neutron flux. For materials characterization, the sample size is typically limited by the amount which can reasonably be synthesized given the available time and funding. This results in an upper limit on most samples of the order of a few cubic cm's. In many cases, researchers wish to measure much smaller sample volumes. There can be many reasons for this, ranging from sample availability and cost to the need to measure local properties in intrinsically inhomogeneous materials. The lower limit to the sample volume is almost always determined by the available neutron flux. Typical beam sizes are therefore in the range of a few mms to a few cms.

4.2.2. Beam divergence

Most neutron experiments are aimed at a measurement of the dynamic structure factor $S(\mathbf{Q},\omega)$ straightforwardly obtainable from the neutron scattering cross-section, or one of its derived quantities such as the static structure factor or reflectivity profile. The dynamic structure factor contains the essential information on the spatial correlations between atoms (as a function of of $\hbar\mathbf{Q}$, the momentum transfer) and their time correlations (as a function $\hbar\omega$, the energy transfer). The spatial resolution which can be achieved depends on the precision with which $\mathbf{Q}$, the wavevector transfer, can be known. Most diffraction measurements will aim to achieve a $\mathbf{Q}$-resolution of the order of 10^{-3} or better in $\Delta\mathbf{Q}/\mathbf{Q}$. This directly results in divergence resolution of $\Delta\theta/\theta$ of 10^{-3} or better, i.e. a beam divergence of the order of 0.1°. Small-angle neutron scattering can generally tolerate a significantly more relaxed $\mathbf{Q}$-resolution, but the need to measure at very low scattering angles near the incident beam, usually also requires a divergence of the order of 0.1°. Spectroscopic measurements will usually accept a relaxation of the Q-resolution in order to gain flux. Todays neutron spectrometers (i.e. instruments for spectroscopic measurements) will typically accept a beam divergence of the order of 1°, and some even 4-5°, in order to achieve the flux needed to observe the desired inelastic signal.

A typical instrument will thus need a phase space volume of the order of 10 (cm-deg)^2 with a few instruments requiring much less and a few requiring up to 20 times as much. For each instrument, a phase space of beam area and divergence at the sample can be specified which the neutron source should fill as completely as possible, in order to maximize flux. Each instrument needs to be equipped with a neutron optical system designed to transport this phase space from the source to the sample, while minimizing the loss of phase space density, in accordance with Liouville's theorem (see AppendixA). Such an optical system usually consists of neutron guides in which the amount of phase space which can be transported is roughly proportional to the neutron wavelength squared, due to the reflection properties of the inner guide surface. As a result, the phase space volume delivered to the sample is usually strongly wavelength-dependent and often only reaches the desired value for longer wavelengths.

In terms of the moderator design, these considerations result in a requirement for the minimum viewable surface area of the moderator. However, the amount of phase which can be extracted from the moderator and the heat load and radiation damage incident on the beam optics decrease with the inverse square of the distance from the moderator face to the entrance window of the neutron optical system. The compromise made at the ESS is to start the guide optics at a distance of 2 m from the moderator center. In order to optimally deliver the typically needed phase space volume of 10 (cm-deg)^2 at this distance, the needed viewable moderator surface can be calculated from simple geometrical considerations to be about 20 cm^2 in area, slightly less for thermal neutrons, slightly more for cold neutrons. More information can be found in [13].

Of the various moderator geometries described here, the TDR geometry provides the largest viewable surface, of the order of 200 cm^2, which is more than adequate for the needs of all the instruments. Optimising the height of the pancake geometry presented a challenge, as the brightness increase obtained by reducing the moderator height is to some extent offset by the reduction in viewable area. A trade-off study was performed between these two effects which is described in more detail in [13], evaluating the impact on the flux at the sample for a full suite of instruments, resulting from the compromise between the increasing brightness of the source and the decreasing brightness transfer of the neutron optical system as the moderator height is reduced. The optimal source height was found to be 3 cm, representing the global optimum for the full instrument suite. Once the optimum moderator height was determined for the pancake moderator, it was straightforward to make the same comparison for the butterfly moderators, which display the same height-dependent brightness. The viewable width of the cold moderator in the butterfly geometry is significantly less than that of the pancake moderator, but this turns out not to be a problem, since the width of the cold pancake is much greater than can be usefully accepted by the instruments guide system anyway. The viewable cold surface area of the 3 cm tall butterfly moderator is approximately 25 cm^2, with some variation with beamport angle. This is sufficient for most instruments. In the case of instruments where a larger area would have been beneficial, the increase in source brightness, compared to the alternative moderators with the larger area, generally more than compensates for the reduced brightness transfer of the system.

The feedback of these phase-space requirements into the moderator design was that the extraction surfaces for both thermal and cold moderators should be at least 6 cm wide. As discussed below, the requirement of bispectral extraction and of the number of beam lines, forced the cold and thermal extraction areas to be adjacent.

4.3. Number of beamlines

The ESS moderators need to permit the extraction of beams for 22 instruments [1]. The instruments are arranged next to each other in experimental halls, such that the beamlines need to be arranged in one or more horizontal fans illuminating the space made available in the halls. Existing facilities typically hardwire the number of instruments into the design of the monolith, by having exactly the number of beamports built into the target monolith corresponding to the number of instruments to be served by the moderators. Given the typical lateral size of neutron instruments and their distance from the target, this has generally resulted in approximately 22 beamports being designed into the monolith, separated by about 12°.

ESS has taken a very different approach, in designing 42 beamports into the target monolith with an average angular spacing of 6°. This creates a grid of beamports, from which the 22 beams needed for the currently foreseen scope of the ESS can be extracted, while the remaining 20 beamports will be sealed with temporary dummy plugs. This has the advantage that the facility layout does not need to be determined for its lifetime by the choice of the initial instrument suite. The monolith design with the 42 beamport inserts

is shown in Figure 7.

The experimental halls of ESS are divided into 4 sectors, of which two (North and East) are similarly sized to existing facilities and will accommodate instruments up to about 60 m in length. The beamports in these sectors have an angular separation of 6° between each. Given the amount of space needed for the instrument components, notably the shielding around the secondary spectrometer, instruments of less than this length will typically need to be separated by about 12°, which will be achieved by activating, on average, every other beamport.

The two other sectors (South and West) can accommodate instruments up to 170 m in length. Even instruments with large secondary spectrometers and shielding can easily accommodate instruments on neighbouring beamports with 6° of angular separation. Integration of components such as choppers in the area close to the monolith on such closely separated neighbouring beamlines does, however, present a significant challenge. In order to keep this difficulty at a tractable level, the beamport separation in the South and West sectors has been staggered to be alternately 5.7° and 6.3°. In this way, each instrument can primarily concentrate on its integration with the neighbouring instrument on the closer beamline.

The ESS design is thus more than sufficient for the 22 instruments foreseen within the current scope of the ESS, and leaves a lot of room for future possibilities.

4.4. Spectral freedom

The source frequency is one of the most fundamental parameters around which all instruments at a pulsed source need to be designed. The choice of 14 Hz as the repetition rate at ESS was made so as to allow each instrument to benefit from a large bandwidth of neutron wavelengths without suffering from frame-overlap, or needing to suppress pulses, as is commonly done on higher rep-rate sources such as SNS or ISIS-TS1. In order to make the most of this available bandwidth, most of the thermal instruments at ESS choose to use cold neutrons as well. This is typically done using a bispectral switch, a device incorporating one or more neutron mirrors at the front end of the instrument's neutron optical system, inclined so as to reflect in cold neutrons from a source to the side of the guide axis. The device acts as a switch because the reflectivity of neutron mirrors is intrinsically wavelength-dependent, so that short wavelengths are transmitted while longer wavelengths are reflected. Without needing to move, it thus switches as a function of wavelength from allowing short wavelength neutrons to be transmitted until the reflectivity cut-off is reached, above which longer-wavelength neutrons are reflected into the guide from the side. Together with the choice of the rather low repetition rate of the ESS, a decision was made early on in the project that all beamports should be able to benefit from the resultant large bandwidth by using bispectral switches. This has far-reaching implications on the design of the facility. Because every beamport can now be populated with a cold, bispectral or purely thermal instrument, every beamport becomes essentially equivalent, and an instruments choice of beamport is no longer based on its spectral needs, as is done at existing facilities

but on other factors, such as the size of the experimental hall behind that beamport, the space allowed by components such as choppers on the neighbouring instruments, or proximity to labs and other important infrastructure.

Currently existing pulsed spallation sources hardwire the spectral characteristic of each beamport into the monolith design by orienting the beamport axis to point at one moderator or another. Adding this new requirement of spectral freedom to all beamports requires a very different approach. Each beamport now needs to be able to view both a cold and a thermal neutron source, which should be placed side by side with the beamport axis oriented at their junction. In this way, the instrument can choose to shift and/or tilt its beam axis with respect to the beamport axis within the envelope given by the beamport insert, so that it points at the cold or thermal moderator. The design of the beamport inserts shown in Figure 7, typically allows the beam to be tilted by about 1° to one side or the other, with respect to the beamport axis.

For the TDR moderator, this works fine. All beamports in one 60° opening should be oriented to point at the junction between the cold and thermal moderators, and the instruments can choose cold, bispectral or thermal beams by tilting one way or the other.

For the pancake moderator, there are two options for achieving this spectral freedom. Each beamport can either be oriented so as to point at the cold-thermal junction nearest to its entrance window or the cold-thermal junction on the other side of the cold moderator. These are known as *near-corner* and *far-corner* extraction, respectively and are illustrated in Figure 26.

Near-corner extraction works well for beamlines near the perpendicular to the proton beam, but results in very low thermal brightness at angles close to the edges of the fan, as the beamport angle approaches the parallel to the thermal-moderator face (see Section 5.1). This is consistent with the known angular dependence of neutron emission from thermal moderators [26]. Far-corner extraction works acceptably well for all beamports, but generally results in lower cold brightness, as the viewing angle of the cold moderator for most beamports results in a reduced depth of parahydrogen being seen. The other problem with the far-corner extraction is that it results in fewer beamports overall, as the beamports near the perpendicular to the proton beam would otherwise clash [13].

The butterfly geometry solves this problem by orienting all beamports towards the nearest cold-thermal junction. For each instrument sector (North, West, South, East), this junction acts as the *focal point* for the beamports, as indicated by the red spots in Figure 25. All beamports can view either the adjacent cold lobe or the thermal moderator on the other side of the focal point, as indicated by the arrows in Figure 26. The butterfly-1 geometry has an advantage over the butterfly-2 geometry for thermal beam extraction, as the central, most intense part of the thermal moderator near the inside of the V-shape is closer to the focal point, making it more readily viewable from most beamports.

4.5. Upgradeability

All three of the studied low-dimensional moderator concepts incorporate a high degree of upgradeability, as two upgradeability aspects were included as design criteria from the outset: firstly the beam extraction geometry has been designed to allow the extraction of many more beamports than needed for the 22 instruments foreseen in the day-one configuration of the ESS. The primary upgrade path of the ESS is to add more instruments to the initial target station, rather than needing to build a second target station, when the 22 instrument slots have been filled, as is the strategy at existing pulsed spallation sources. This is a far more cost-effective upgrade path, capitalizing on the high performance of the existing accelerator and target station, without the large added expense of a second target station and the dilution in proton beam power associated with the need to supply beam to two target stations with the same accelerator. In order to facilitate such an upgrade, the angular separation of the beamports at ESS has been set to about half that of existing pulsed spallation sources, resulting in up to 42 possible beamports, see Figure 7.

Secondly, the design requirement that all beamports can freely choose between viewing the cold and thermal moderators provides a significant additional freedom of choice when placing future instruments. In addition, contrary to current pulsed spallation sources which use a combination of coupled, decoupled and poisoned moderators to provide the range of pulse-width characteristics needed by the instrument suite, the ESS as a long-pulse source, provides a much greater range of pulse widths by tailoring the source pulse on an instrument-by-instrument basis using pulse-shaping choppers on all the beamlines which need them. This range is available to all instruments, both for day-one instruments, and for instruments which are part of a future upgrade. Finally, by allowing all the instruments to be served by the same moderator assembly above the target, the space for moderators below the target is kept free to be used for future developments. Some ideas are briefly discussed in the conclusion section, as well as in Ref. [13].

One aspect of the target station design which does impose limitations on future moderator designs is the location of the four focal points. The focal points are intended to be fixed for the lifetime of the facility, as the beamport inserts are integrated into the whole target-monolith system. The height of the beamport inserts is set so as to allow a neutron beam to be extracted from either the top or the bottom moderator, or even both. The horizontal coordinates of the focal points thus apply equally to both the top and bottom moderators and are fixed for the lifetime of the facility.

4.6. Iterative procedure for moderator optimization

The considerations outlined above for optimal beam extraction need to be incorporated into the design of the moderators. At ESS, this was approached in an iterative fashion. The requirement on the viewed surface at the moderator, for the ESS beam extraction configuration, was that a width of at least 6 cm was needed, for both thermal and cold extraction surfaces [13]. Such a width should be seen from each of the beamports, and was therefore treated as a requirement for the moderator design.

Figure 12. Calculated brightness B_{0-20} map on the emission surface of cylindrical moderators of different heights: 1.5 cm (top), 3 cm (center), and 10 cm (bottom).

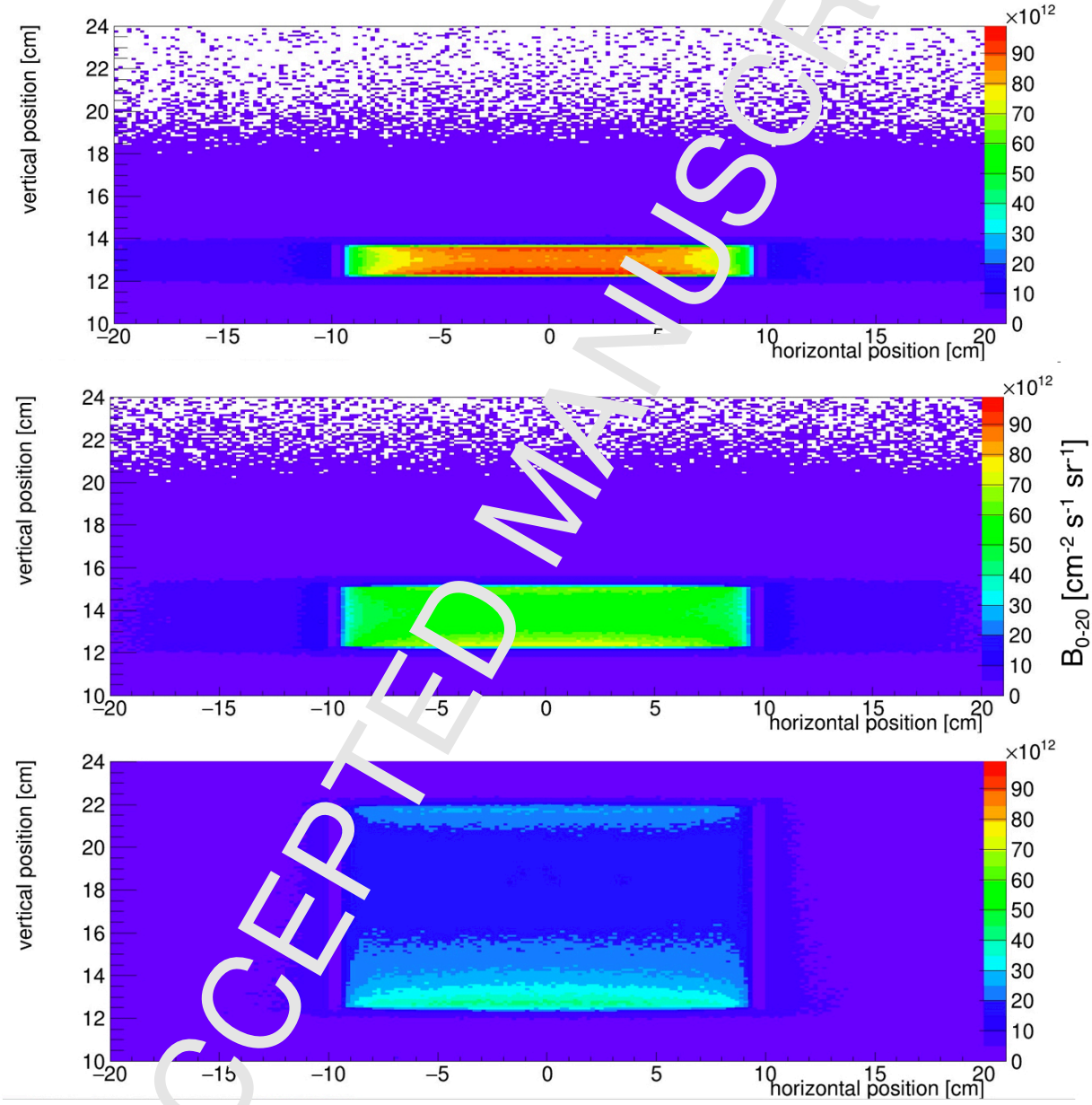

Figure 13. Same as Figure 11 for B_{0-20}.

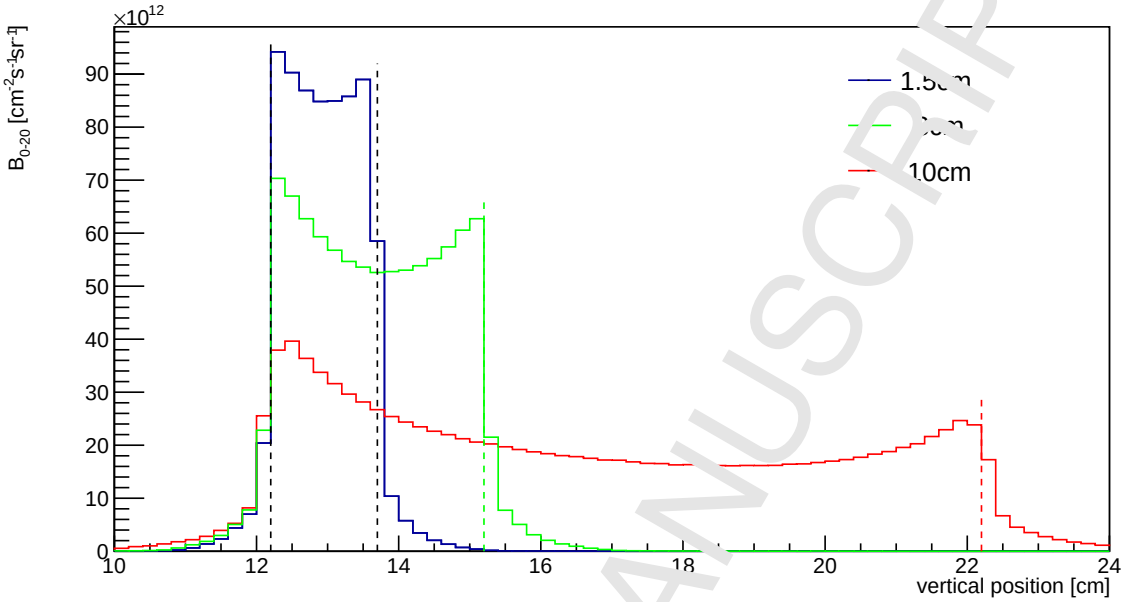

Figure 14. Same as Figure 11 for B_{0-5}.

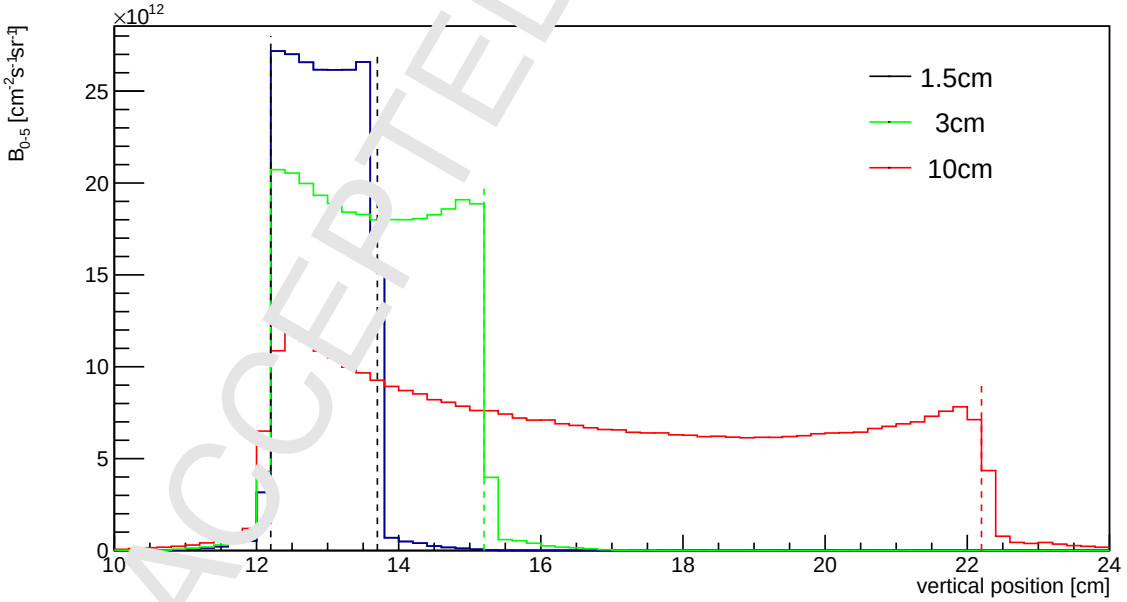

Each moderator design as it was proposed to the instruments was evaluated for performance impact on each instrument, and the result was fed back to the moderator design team. At each iteration, the strengths and weaknesses of each particular moderator design for instrument performance were highlighted, allowing an informed adaptation of the design to the instrument needs. This allowed the optimal moderator height to be calculated, so as to maximize the global performance of the instrument suite. The issues related to beam extraction were also evaluated at each iteration, culminating in the butterfly moderator geometry which takes all the relevant performance parameters into account.

According to these criteria, the chosen moderator height was 3 cm for both thermal and cold moderators.

5. Moderator Design Choice

5.1. Relative performance of the different concepts

In this section we compare the performance of the three concepts considered for low-dimensional moderators. The brightness was calculated from a viewed surface of the moderator 6 cm wide, 3 cm high. This was done for both thermal and cold moderators and the requirement in the calculations were that each viewed surface would be at a distance of at most 1 cm from the focal point.

For the pancake, the dimensions of the cold hydrogen disk that gave the highest cold brightness was chosen, for both near and far corner extraction.

For the butterfly-1 and butterfly-2 moderators, the total length of the moderator system (along the proton beam axis), after optimization, is of 24 cm and 28 cm, respectively. For the pancake, the optimal diameter of the cold moderator disk is 20 cm, for both near- and far-corner extraction. The overall pancake moderator is, however, wider than both butterfly-1 and butterfly-2, as the 6 cm wide thermal extraction areas must be considered, on both sides of the cold moderator, making the full pancake moderator system about 32 cm wide.

The Monte Carlo models do not have full engineering details, as they were not available at the time of performing the optimization study. However, in an attempt to estimate absolute values of the brightness expected, several details are included such as pipes, correct material thicknesses, and gaps, while some materials are mixtures in order to take into account water loops for cooling, or flow guides in hydrogen or water moderators.

The three low-dimensional designs (one pancake and two butterflies) had exactly the same level of engineering details, allowing a proper comparison of the different concepts. The target, reflector, and all the surrounding of the moderators were identical, and the only difference between the models were the thermal and cold moderators inserted. The flow channels inside the moderators were not modelled, instead the material inside was a mixture of parahydrogen with 5% of aluminum to take into account the reduction in performance due to the presence of alumimum flow guides inside the moderator vessel.

In the case of the TDR volume moderator, in order to perform as fair a comparison as possible to the other models, we took the model used for the TDR work, and added some engineering details (e.g. same structure and amount of cooling water in the reflector) to make it similar, from the engineering point of view, to the latest low-dimensional models. We also considered the same type of beam extraction, i.e., within 7 cm from the focal points, placed at the intersection between thermal and cold sources, as for the latest models.

Despite the addition of engineering details, this updated TDR model is probably still favored with respect to the other concepts. Since the publication of the TDR, the spallation target has been redesigned in favour increasing the volume for the flow of the helium coolant, and the moderators have been moved further away from the target to increase the safety margins. These changes result in a reduced neutronic performance close to 10 %. They have not been incorporated in the updated TDR model presented here.

Figure 27 shows the resulting brightness angular distributions within one 120° sector of ESS for the low-dimensional moderators considered. Due to symmetry, the results are identical in the other sector. Integral thermal B_{20-100} and cold B_{0-20} brightnesses are shown for the pancake geometry (with near-corner and far-corner extraction) and for the two butterfly configurations.

Table 2 lists the average integrated thermal and cold brightness for the designs considered. From Table 2, it is apparent that all the low-dimensional models have a much higher brightness than the TDR, thus justifying the transition from TDR to low-dimensional moderators.

Of the two beam extraction concepts for the pancake geometry, the far-corner option is preferable, as it offers a larger gain in thermal brightness, though it results in the loss of a number of beamports. Reduction of each pair of beamports can be seen as a loss of available neutrons to the facility, considered as whole, of about 5%. The near-corner extraction option for the pancake provides a higher cold brightness and does not result in a reduction in the number of beamports. The thermal brightness, however, falls to unacceptably low levels for the edge beamports.

The two butterfly concepts were designed with the goal of increasing the thermal brightness, maintaining (or increasing) the high cold brightness, and easing the beam extraction. Of the two concepts, the most successful is the butterfly 1, because; *i*) it has the highest cold brightness of all concepts. More than two thirds of the instruments of ESS are cold or bispectral, therefore in the overall figure of merit to choose the best concept, cold brightness must have the priority. *ii*) It has the second best thermal brightness, after the butterfly 2, which however has a significantly lower cold brightness.

Compared to the pancake with far-corner extraction, the butterfly 1 gives both higher thermal and cold brightness (factor 1.13 and 1.12, respectively), without the problem of the loss of beamports. The real gain is however higher, considering the higher number of beamports available for the butterfly 1 concept, as discussed. Compared to the pancake with near-corner extraction, it gives a slightly higher cold brighness, and an average thermal brightness higher by a factor of 1.47.

Figure 15. B_{20-100} distribution across the moderator height, for thermal neutrons. Neutrons are extracted from the water-filled sides of three moderators of cylindrical geometry, with 1.5 cm, 3 cm and 10 cm height.

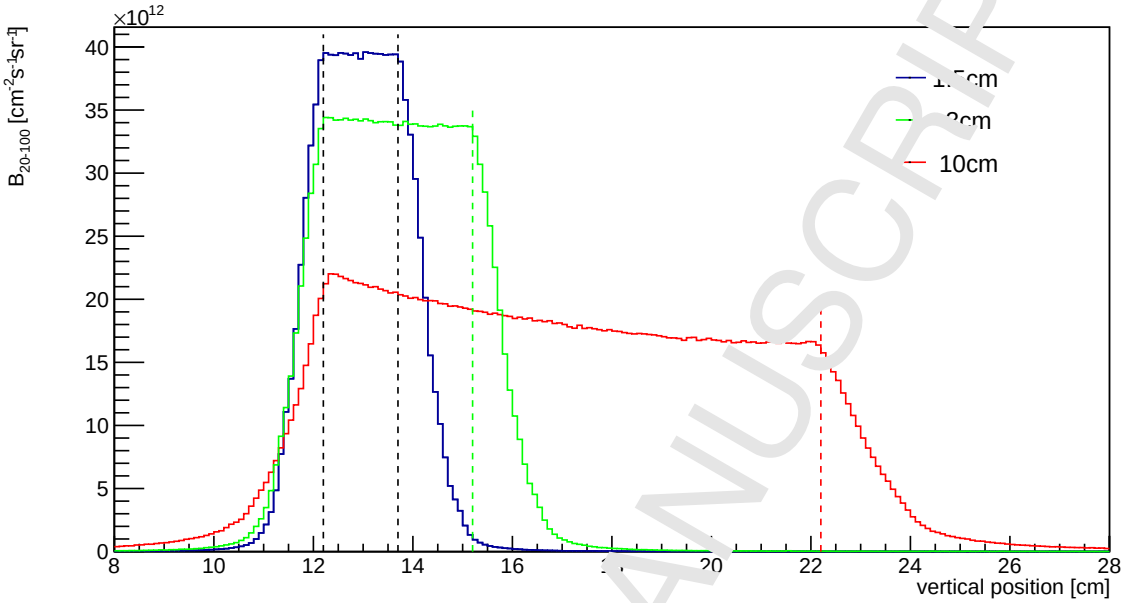

6. Description and performance of the butterfly 1 moderator

The first moderator that will be installed at ESS at the start of the facility will be a butterfly 2 moderator, which was initially chosen mainly because of the higher thermal brightness. At the time of writing, a detailed engineering design has been finished and the moderator is in fabrication for installation in 2021. For a final configuration of the top moderator we decided to adopt a butterfly 1 design, for the reasons outlined in Section 5. The instruments and their beam extraction systems are designed for that moderator. The butterfly 1 system will be installed in the early years of ESS during the power ramp-up. That is why detailed engineering models are not yet available for the butterfly 1 system.

In this section we give a full description of the butterfly-1 moderator chosen for ESS. The geometry of the butterfly moderator is shown in Figure 25. Engineering details have been extrapolated from the existing engineering model of the butterfly 2 [27].

The MCNPX model of the structures surrounding the moderator is shown in Figures 28 to 30. Some important details of the model are the following:

- The tungsten target was modelled according to the engineering drawings. The density of the tungsten used in the model is of 15.1 g/cm^3, corresponding to the effective density deduced from the engineering design, which consists of tungsten bricks with cooling gaps, for a filling factor of tungsten of 78%. The

Figure 16. Angular distribution of propagation direction with respect to the horizontal plane of cold neutrons ($E < 20$ meV) emitted from the surface of the parahydrogen moderator.

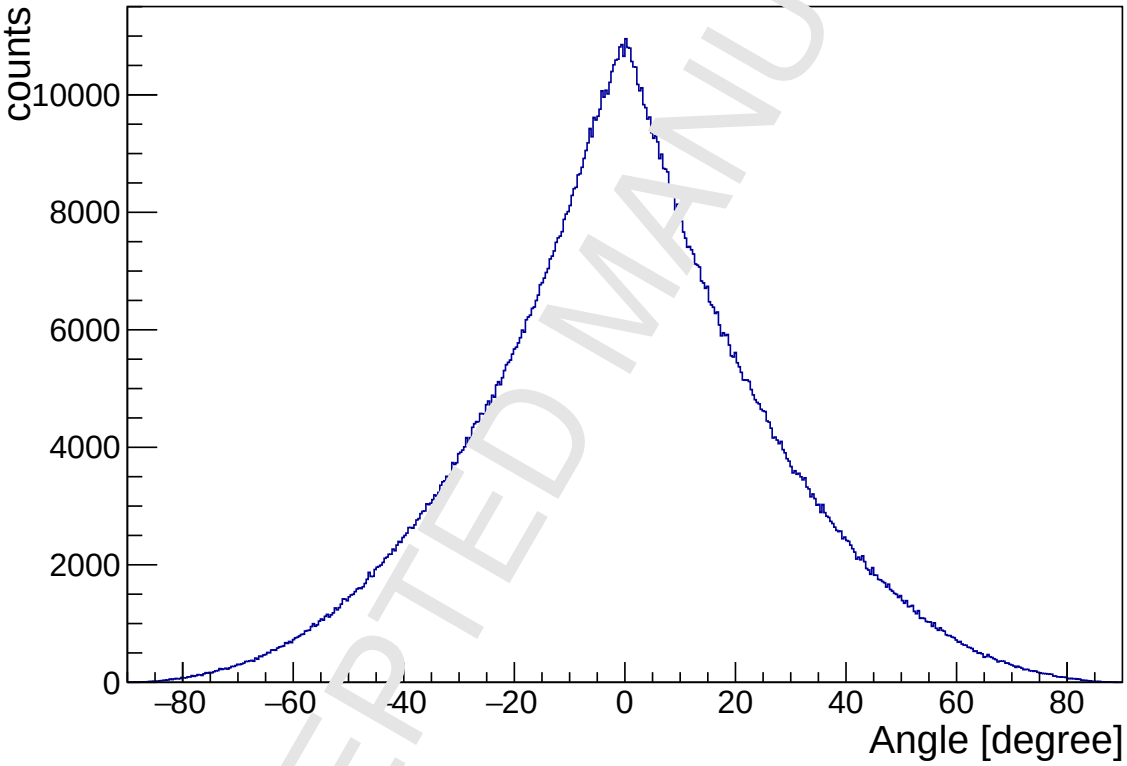

Figure 17. Angular distribution of the propagation direction with respect to the horizontal plane of thermal neutrons (20 meV $< E <$ 100 meV) emitted from the surface of the water moderator.

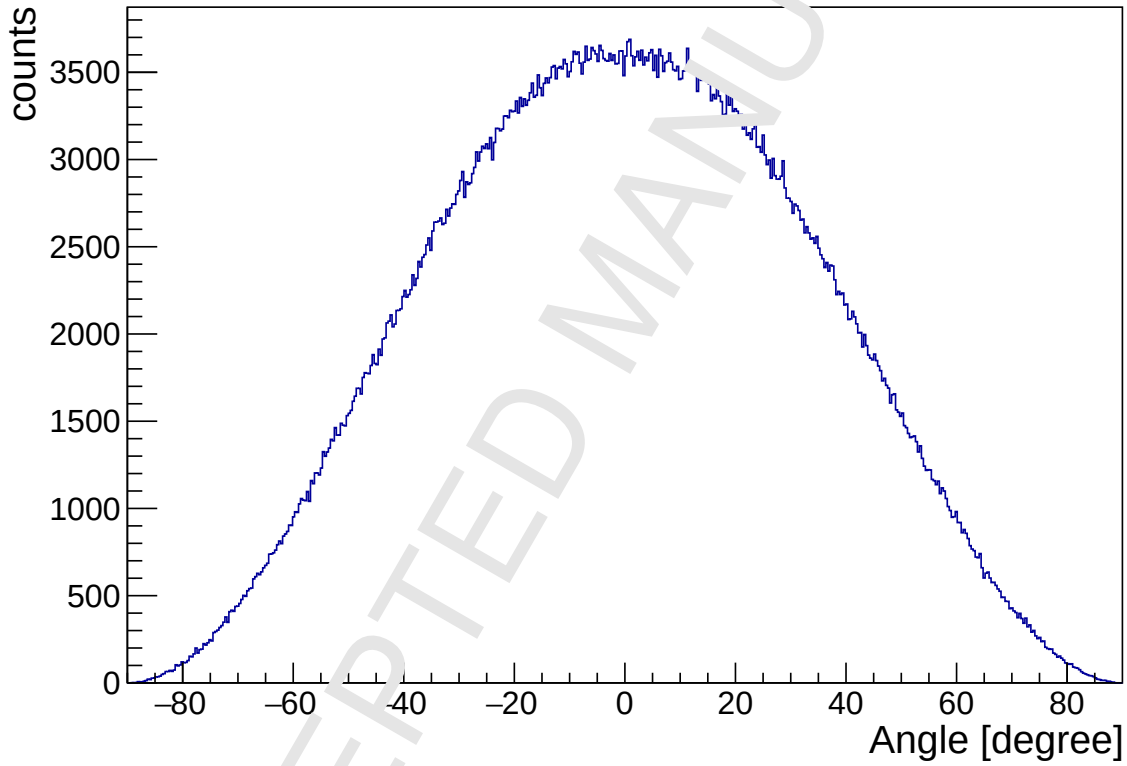

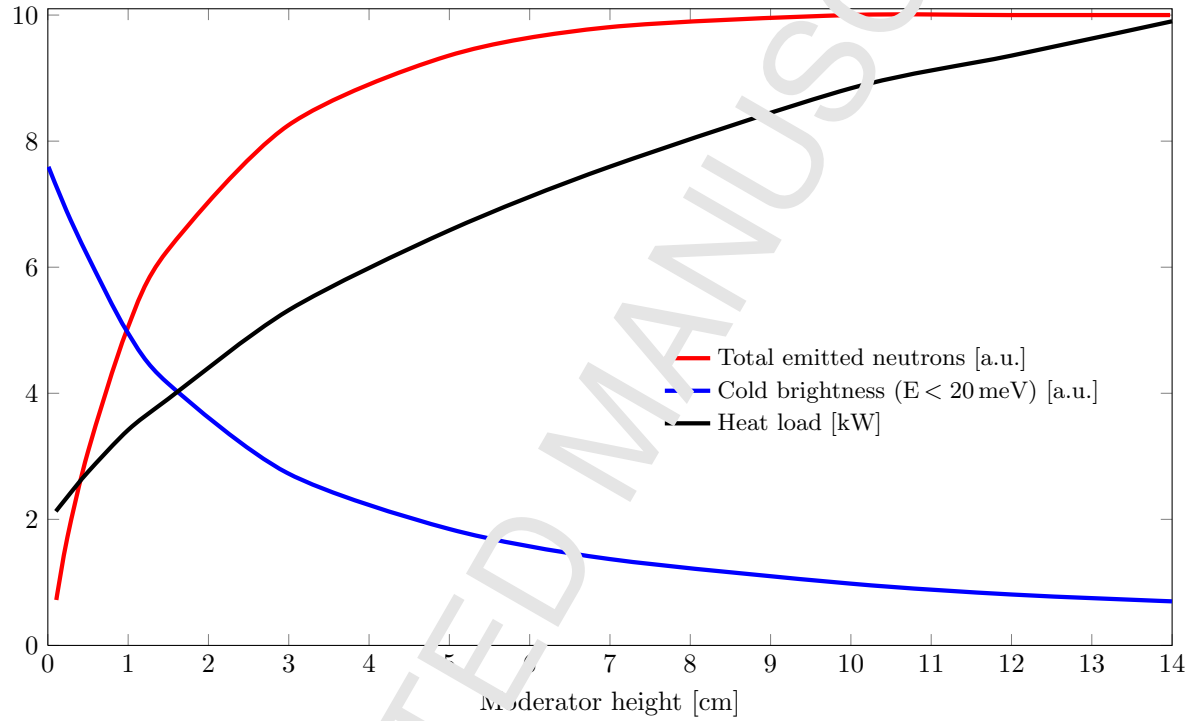

Figure 18. The integral cold brightness B_{0-20} increases with decreasing height of the moderator. On the other hand, the total number of emitted cold neutrons (B_{0-20} multiplied by the viewed area of the emitting surface) and the heat load both increase with the moderator height. The heat load is calculated on the cylindrical aluminum vessel and on the pure parahydrogen inside, without piping or other engineering details.

Figure 19. Relative change in thermal and cold brightness as a function of the premoderator radius, for two configurations, in which the ring outside the premoderator (with inner radius equal to the premoderator radius, and outer radius of 60 cm) is void, or beryllium with 30 vol% water.

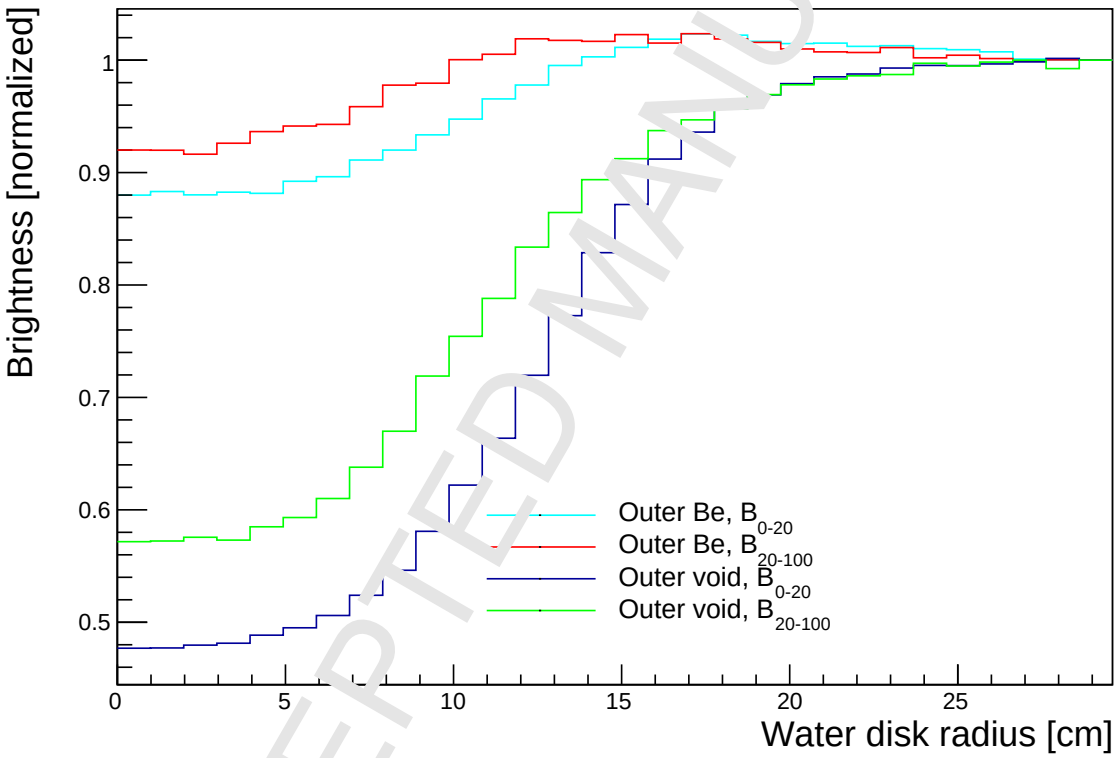

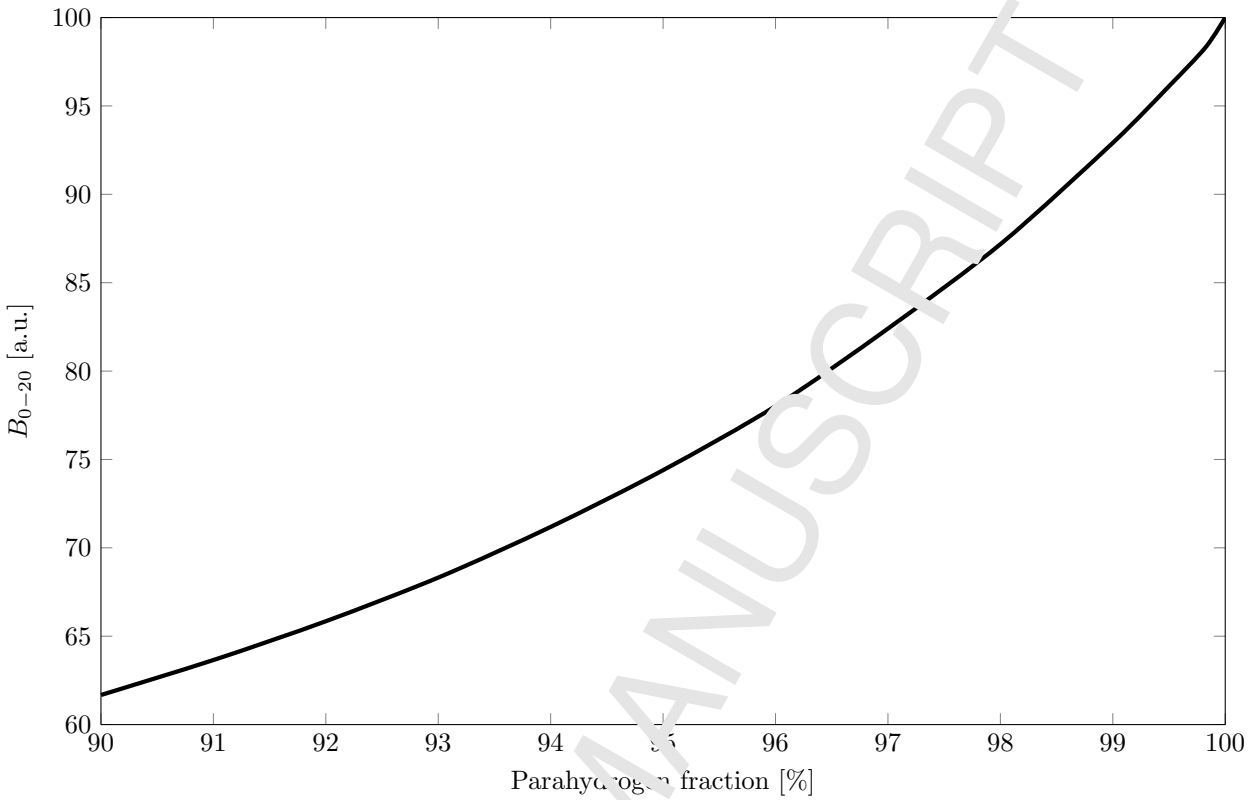

Figure 20. Brightness B_{0-20} relative variation, for the 3-cm high cold moderator, as a function of the parahydrogen fraction, calculated using the ENDF-B/VII cross section at 15 K.

Figure 21. Map of high-energy ($E > 0.1$ MeV) neutrons crossing a horizontal plane located between the tungsten target and the premoderator, at Z=8 cm. The shape of the butterfly (left) and pancake (right) moderators are superimposed. (The proton beam direction in the figure is upward.)

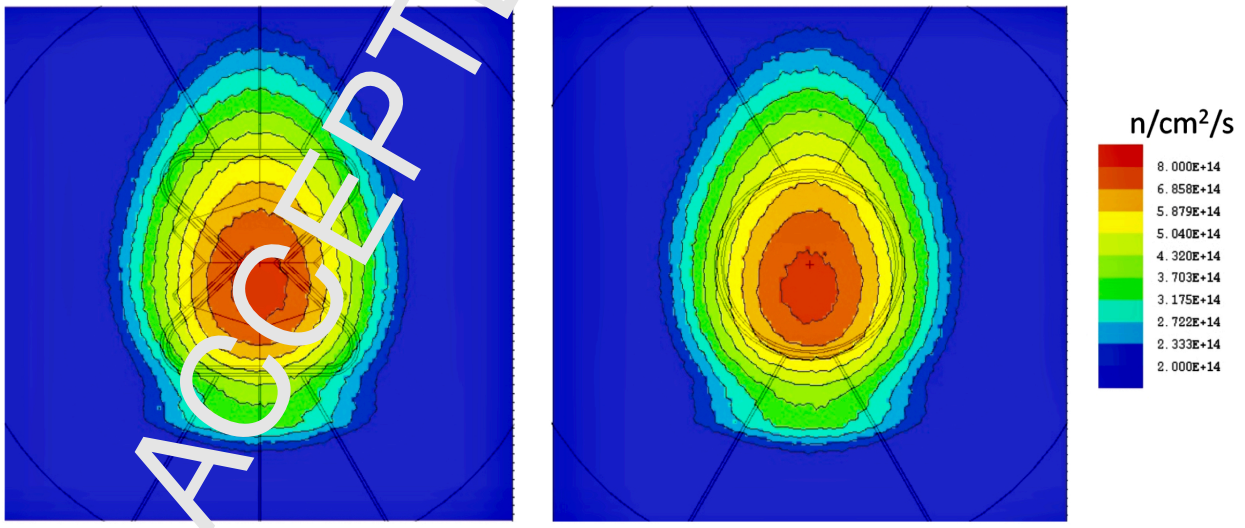

Figure 22. The fast neutron emission distribution for the 1.5, 3 and 10 cm tall pancake moderators The results have been obtained by a point detector tally (f5) with the emission position (horizontal axis, 0=center of target) calculated by extrapolating the trajectories back to the center of the moderator. Neutrons shown as starting outside the window defined by the moderator edges (dashed vertical lines) traverse through the structure around the moderator that is aligned to the physical edges of the moderator volume.

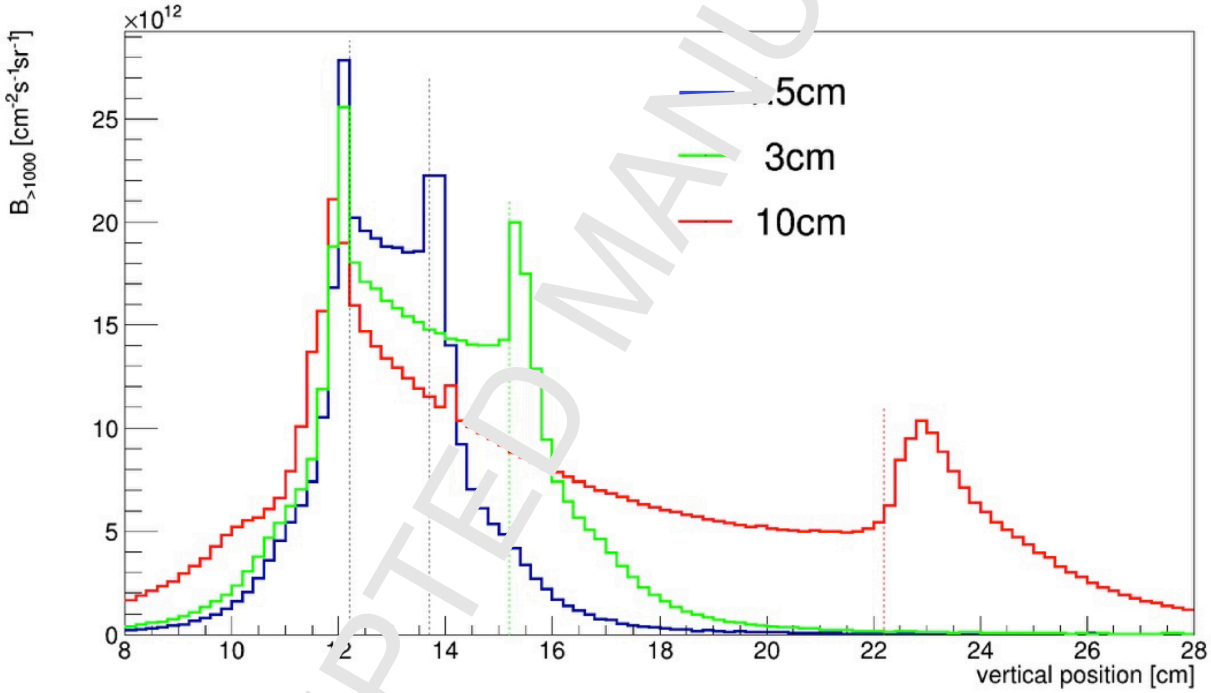

Figure 23. Evolution of the relative signal to fast neutron background ratio (S/B_F) and the data collection figure of merit (FOM) as a function of moderator height. For definitions see the text in Section 2..

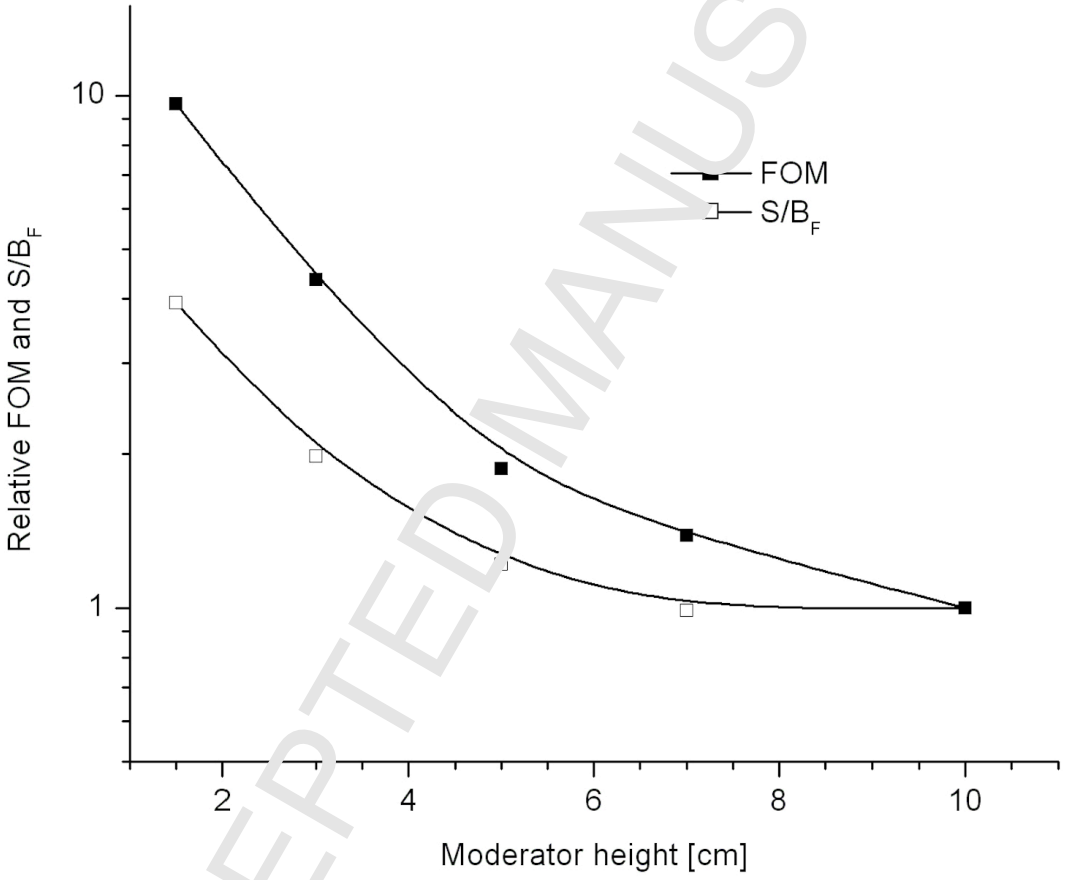

final brightness was calculated using a model with the individual bricks, and it was verified that it gives the same brightness as the homogenized model. The SS316L container of the bricks was modelled in detail according to the engineering drawings.

- The water premoderator between target and moderator consists of an aluminum vessel, containing a mixture of water and aluminum, with a volume fraction of Al of 8 vol% to account for water flow channels, deduced from the engineering drawings of the water premoderator currently in construction.

- Similarly, parahydrogen in the cold moderator contains 5 vol% of aluminum, corresponding to the expected volume fraction occupied by the flow channels. The final model however contains a preliminary design of the flow channels [28]. The shape and thickness of the aluminum vessel is modelled according to the engineering drawings.

- Thicknesses of aluminum walls of the cold and thermal moderators, and of the beryllium reflector are in agreement with the engineering drawings. Similarly, the beryllium reflector is modelled according to the present status of the engineering design, with the expected amount of light water cooling.

- The outer reflector is made of SS316L with 10 vol% of water cooling.

- Two hydrogen pipes, inlet and outlet, are assumed for the cold moderator, see Figures 25 28 and 30

The results provided are with a fast neutron reflector placed at the bottom of the target. For the first moderator-reflector plug, with a butterfly 2 moderator at the top, a steel plug is designed for the bottom, which gives a 4 % brightness increase with respect to having a two-moderator configuration. The result presented here are for a reflector providing a 9 % brightness increase which could be achieved by a water-cooled beryllium or copper reflector, while a better performance could be obtained using other options, such as helium cooled tungsten (cf. Table 1).

6.1. Focal points

The focal points are different for the four instrument sectors. The focal points are (for the North sector) X=5.4 cm, Y=8.9 cm, Z=-3.7 cm. For the other sectors, the absolute values of the X and Y coordinates are unchanged, but the signs change according to the sector (see Figure 25).

6.2. Horizontal viewed width

Figure 31 shows the projected widths at the moderator surface, for thermal and cold moderators, for the different beam ports. In general there is a good balance between maximum widths of thermal and cold moderators, as required for effective beam extraction.

6.3. Horizontal brightness distributions at moderator

In Section 2 the brightness distribution along the height of the 3-cm pancake moderator was shown for several integrated brightnesses. The shapes of these distributions depend mainly on the moderator height and therefore the vertical distributions for the butterfly moderators are similar (while the absolute values depend on the performance of the moderator).

Horizontal distributions of the brightness at the moderator surface were also calculated. This work was part of a detailed characterization of the moderator brightness, being used in the ray-tracing code McStas [29], for guide and instrument design.

The geometry and brightness data presented here have been implemented in the most recent version of the McStas ESS source component, released as an updated component library for McStas 2.3. The implementation is based on functional fits to the underlying MCNP data. This approach ensures that the simulations run efficiently, but comes with some simplifications and assumptions, which means that the results are only valid to within about 10%. Users which are willing to accept a CPU performance penalty, can instead make use of the MCPL implementation [30], where MCNP neutrons are individually handed to McStas with no loss of accuracy in the transition between codes.

Horizontal distributions were calculated with MCNP using collimators placed at 3 m distance from the moderator, looking at a surface 2 mm wide, 30 mm high, moving the collimator to obtain a distribution across the thermal and cold moderators. Results are shown in Figures 32 and 33.

The brightness distribution across the viewed surface shows variations for different beamports. For example, for the W1/E1 beamports, the cold brightness is low for about two cm from the focal point, then it reaches a plateau about 5 cm wide. This is due to the lower amount of hydrogen viewed at this particular angle, for that 2-cm window (cfr. Figure 32). Figure 33 corresponds to a beamport at 42° with respect to the proton beam axis, which is very close to the 45° angle of of the cold moderator vessel walls adjacent to the thermal moderator. Therefore this beamport sees for a few cm of the extraction window the cold vessel in its entire length across that diagonal, resulting, for about half of the viewed surface, in a brightness about 25 % higher than for the other half; if neutrons are extracted from that 3 cm window only, the cold brightness would be about 12 % higher than from a 6 cm wide window.

Thus, for the cold moderator, a significant gain of 10-15 % is observed for 16 out of the 42 beamports. Such effects are not possible for the pancake, nor for the butterfly-2, and if exploited by careful guide optics design it can yield an additional cold brightness increase for several beamports.

6.4. Brightness results

In Figure 34 the distribution of B_{0-20} and B_{20-100} for the 42 ESS beamports is shown. For 16 beamports we observe a significant increase of the cold brightness. These are the beamports where the quasi-tube

Figure 24. The TDR configuration. *Left*: Vertical cut showing top and bottom moderators. *Right*: Horizontal cut showing top cold moderator and water extensions for bispectral neutron beam extraction.

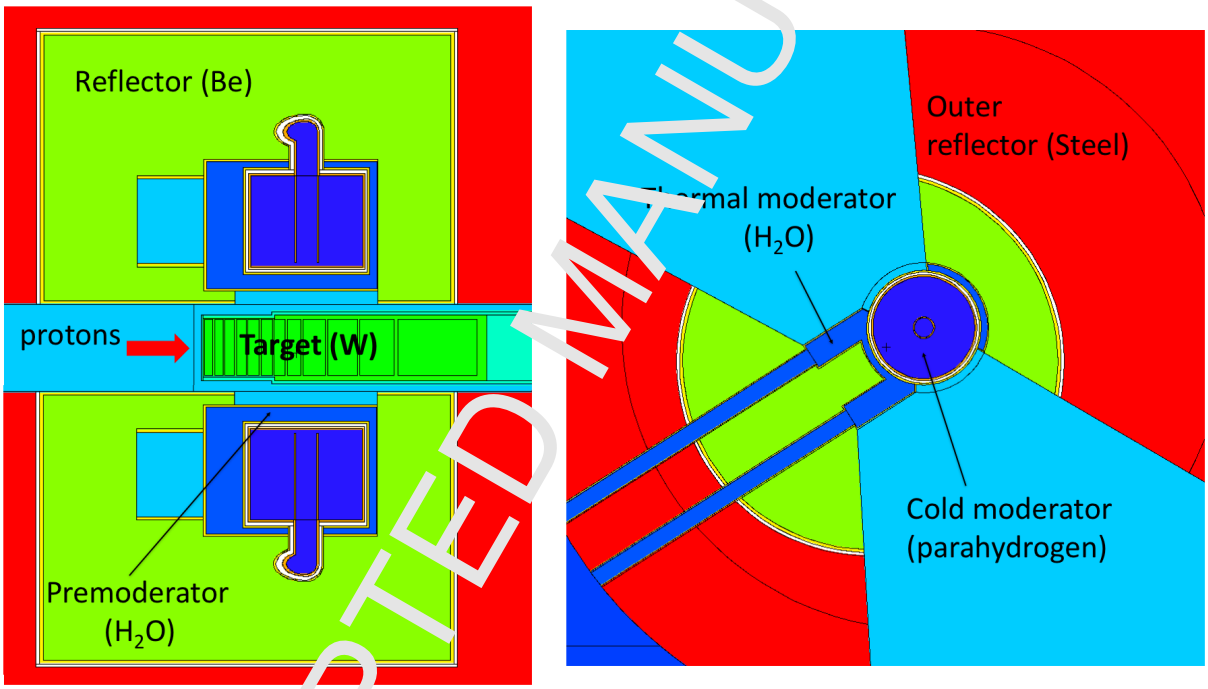

Figure 25. MCNPX models of the two butterfly designs. *Top*: butterfly 1 design, with a single cold moderator vessel and light water moderators, all placed above the neutron production hot spot. *Bottom*: butterfly 2 design, where the cold moderator is split in two parts, and the water moderator occupies a major part of the hot spot. The focal points, the origin of the beamport inserts, are indicated for both designs with red dots.

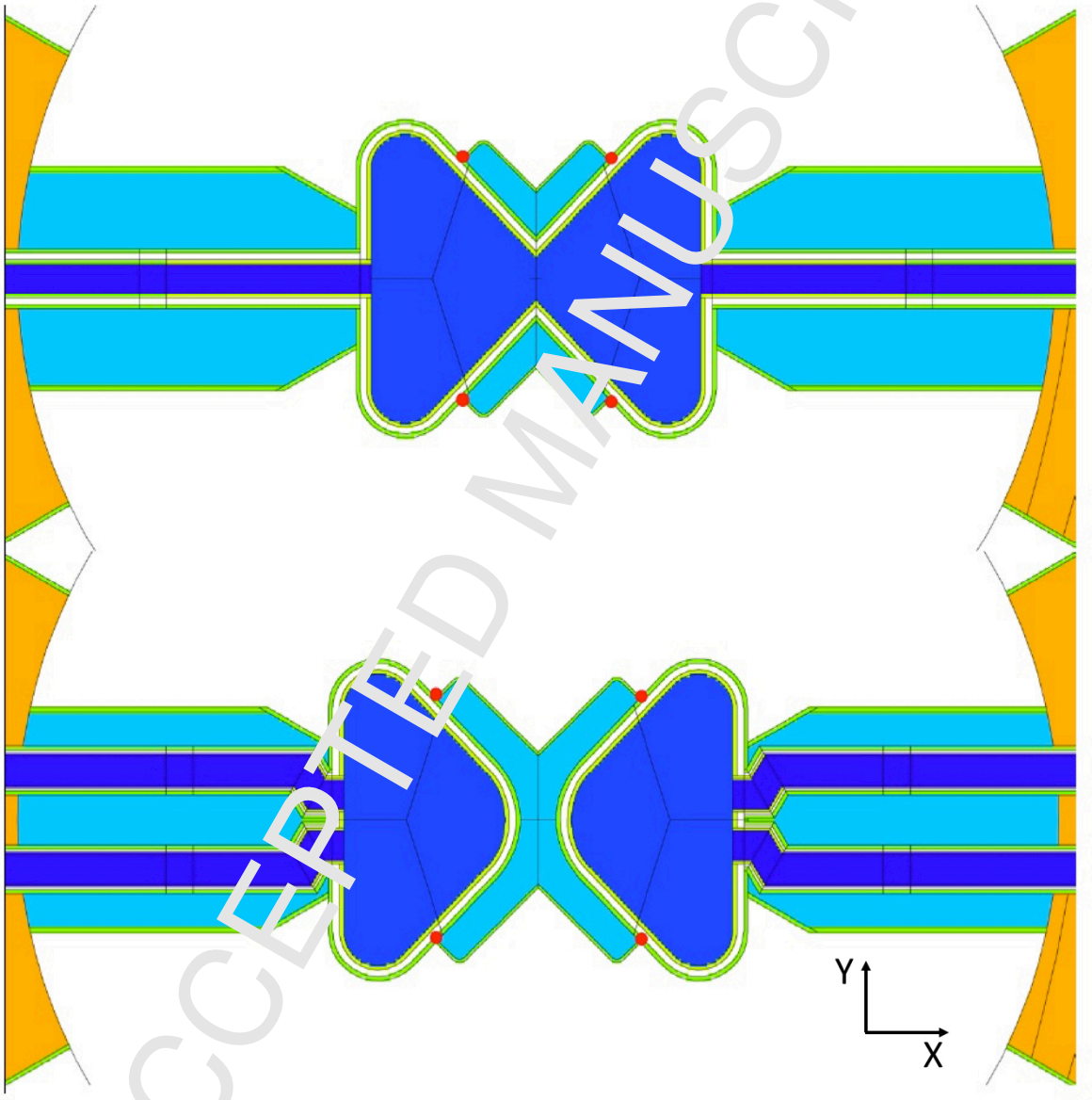

Figure 26. Schematic view of the different beam extraction configurations for thermal (red arrows) and cold (blue arrows) neutrons for the pancake and butterfly moderator. For the pancake, near-corner extraction (*top left*) and far corner extraction (*top right*) are possible. For both butterfly concepts, near corner extraction is used (*bottom left and right*). The red dots show the beamline focal points.

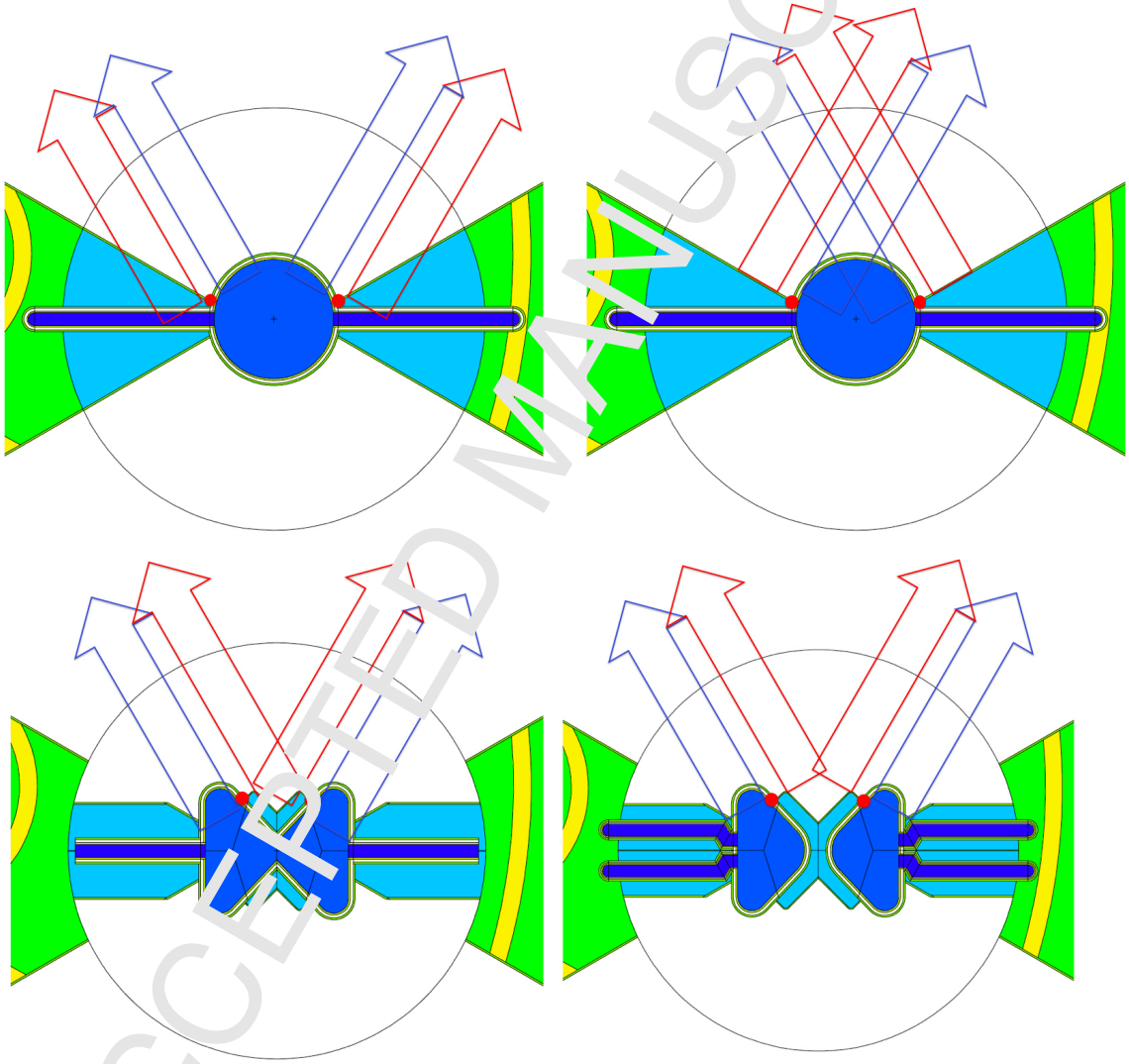

Figure 27. Time-average integrated thermal and cold brightness for the beamports in the South and East sectors. Thermal brightness B_{20-100} integrated between 20 meV and 100 meV. Cold brightness B_{0-20} integrated between 0 and 20 meV. The horizontal viewed width at the moderators is 6 cm.

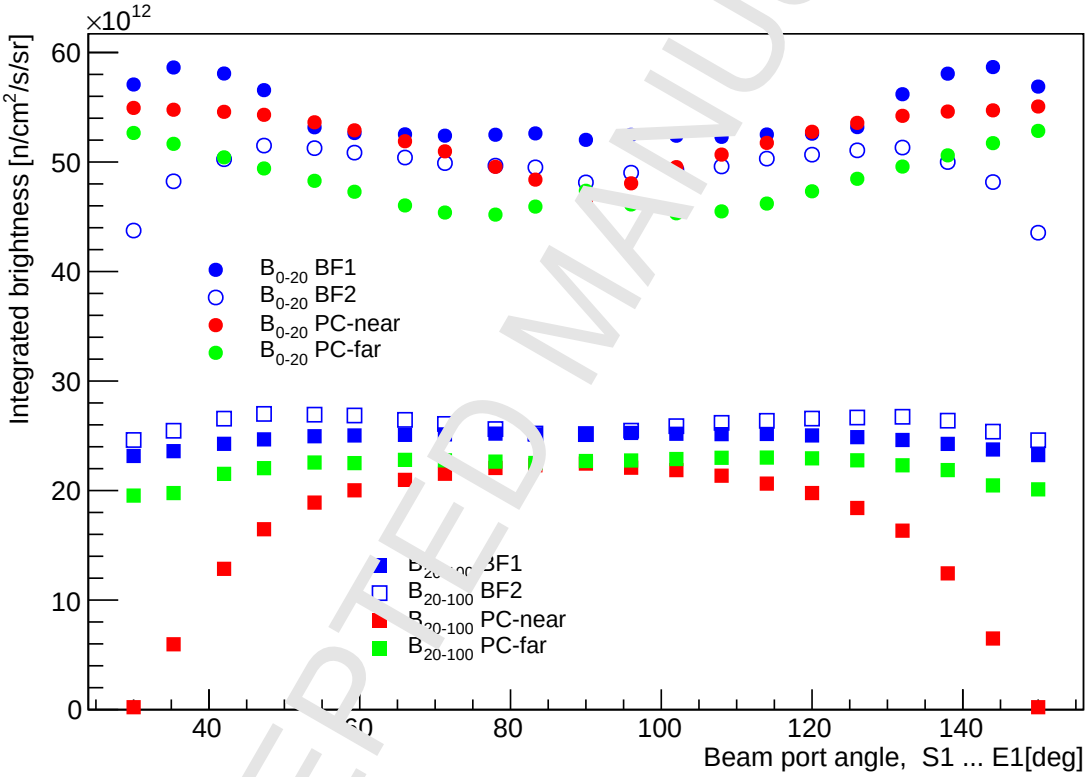

Figure 28. MCNPX geometry used for the brightness calculations of the butterfly 1 moderator, side view. Proton beam comes from the left impinging on the tungsten target. The spallation target contains tungsten bricks (green) nominal density of 19.3 g/cm^3, except for the last two rows which contain stainless steel bricks. However some calculations were performed using a single cell with density of 15.1 g/cm^3 to account for the fraction of helium in the target according to which the filling factor of tungsten is 78 vol%. The water premoderator (light green) between target and moderator has a 8% volume fraction of Al, to account for flow channels, not modelled. The beryllium reflector (light blue) includes water channels (light green) according to engineering drawings. The outer reflector (orange) is made of stainless steel, with 10% volume fraction of water, for cooling.

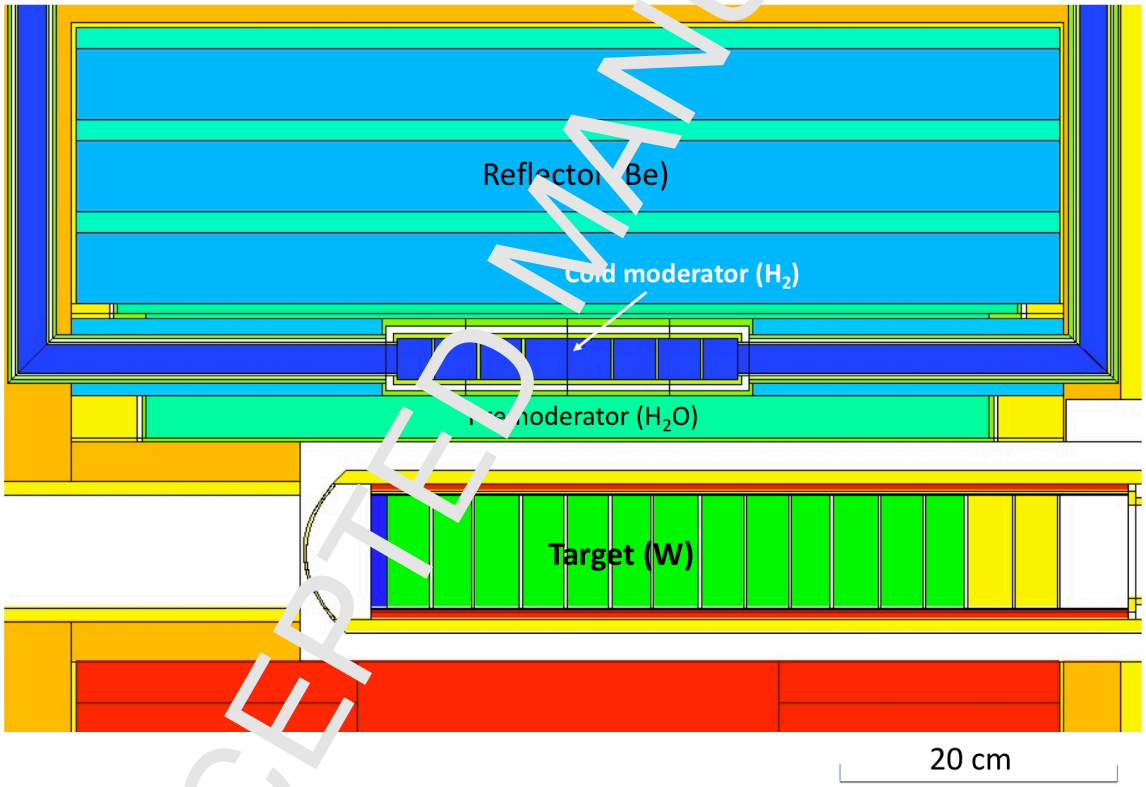

Figure 29. MCNPX geometry used for the brightness calculations of the butterfly moderator, side view showing beam extraction channels. The proton beam is entering the figure in correspondence to the central area of the target.

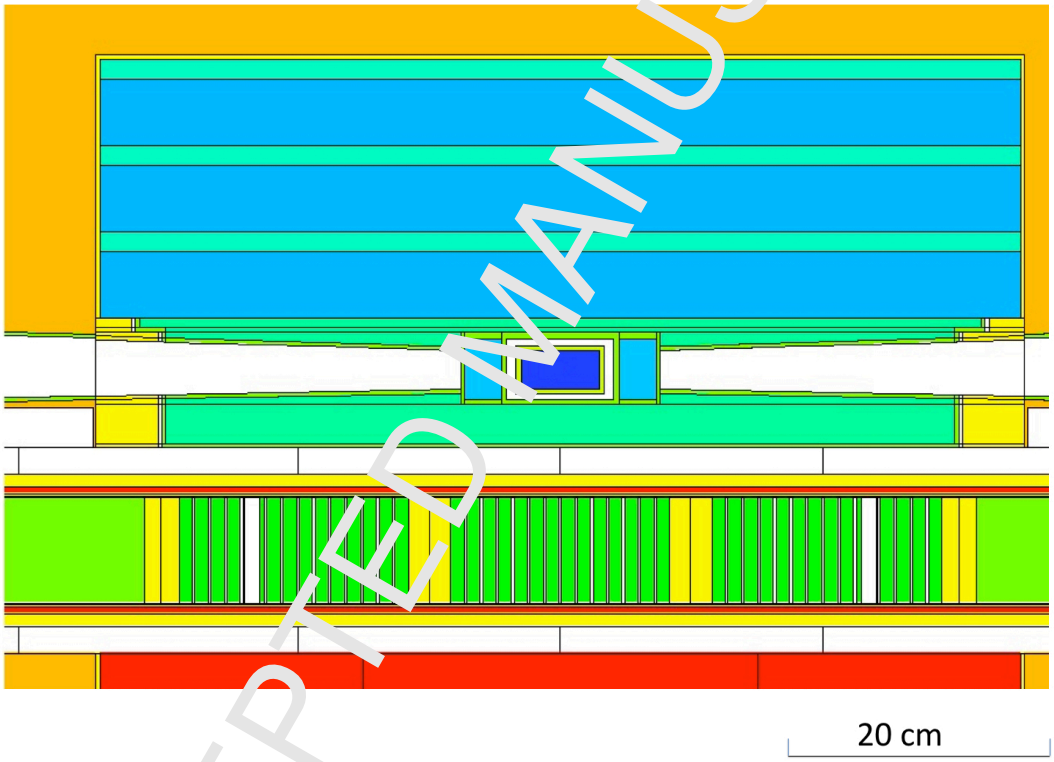

Figure 30. MCNPX model of the butterfly 1 moderator with modelled flow chann[illegible] [28]

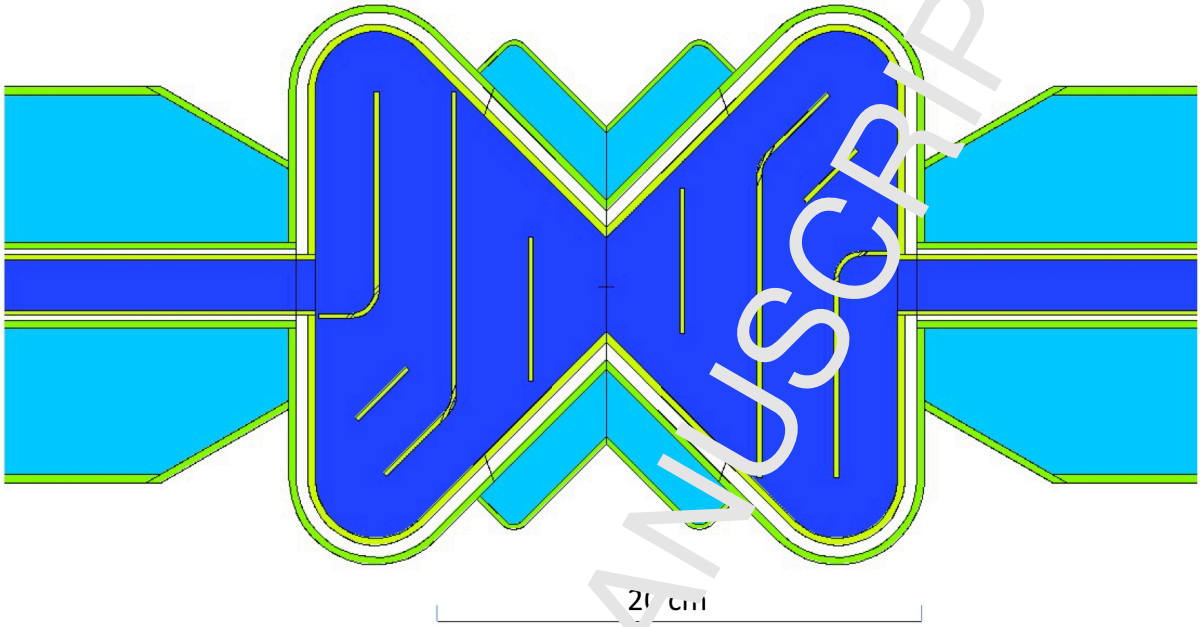

behaviour of the moderator is present. On the other hand, the thermal brightness does not shown a strong dependence on the beamport location.

Figure 35 shows the thermal and cold peak spectral brightness, averaged over the 42 beamports. The shapes of the thermal and cold spectra are essentially the same for all the beamports, which justifies taking the average.

The distribution of the time averaged integrated brightness for the butterfly 1 moderator with all the available engineering details is shown in Figure 27.

When optimising the guide design for an individual instrument, a two-stage process is recommended. Firstly, the instruments guide should be oriented within the beamport insert to point at the centre of the relevant source: for a cold instrument, that is the centre of the circle defined by the circular arc defining the nearest lobe of the hydrogen moderator. For a thermal or bispectral instrument that is the centre of the V-shape of the outside surface of the thermal moderator.

The exact orientation should then be refined using the McStas source component to maximise the instrument performance. The effective brightness of the source will vary by up to about 15% depending on the width and angular acceptance of the guide system.

The performance of the ESS source can be compared with the official ILL brightness values from the

Yellow Book [4]. The original design goal of ESS was to achieve a cold peak brightness 30 times the average ILL brightness [1]. As shown in Figure 36, with the present design using low-dimensional moderators, we are far above this goal. The cold brightness of the butterfly 1 moderator is (at 4 Å) about 150 times higher than the yellow book value. The thermal brightness at 1.5 Å is about 8 times higher than ILL[1]. Similar ratios are found for the integral values in the ranges considered in this work (cf. Table 2).

The brightness results of Figures 35 and 34, and the numbers in this Section refer to the presented design of the moderator-reflector system. The engineering design is ongoing and changes to the final design will affect the moderator performance. The results are given assuming the presence of a fast neutron reflector below the target giving an increase of 9 % in neutronic performance of the top moderator, compared to having a second moderator assembly below the target (see Table 1). A lower performing reflector, or the presence of a bottom moderator similar to the top one (i.e. with a water premoderator) would reduce the brightness by some %. It will be a strategic decision to be taken at a later stage, whether to focus on the top moderator or to consider different sources at the bottom moderator, which will depend on several factors, including the proposal of novel source concepts. If priority will be given for many years to a high performing top moderator, it will be worth considering an optimized fast neutron reflector which would give a further increase in performance of the top moderator.

6.5. Absolute uncertainty

A question arose during the design phase, of a possible higher impact of the engineering reality on the neutronic performance of the low-dimensional moderator, with respect to a volume moderator, that would decrease the brightness gain in a real situation. This was studied in detail, also because before deciding on a single butterfly-1 moderator, detailed engineering for a configuration of two butterfly-2 moderators, one 3 cm high, the other 6 cm high, was performed. This allowed to monitor the impact on the brightness of the two moderators, when engineering details were progressively added to the model. It was found that the relative performance of two moderators with significantly different heights (3 cm and 6 cm) does not change in the transition from physics models to models with added engineering details. This result is consistent with the values from Table 2 that compare the updated TDR model to the low-dimensional moderator engineering models.

Although the full engineering design of the butterfly-1 has not yet been performed, an attempt to include all the engineering details (and associated penalties in neutron production) was made in agreement with the

[1] According to a recent unpublished compilation of experimental and computational data, the ILL brightness should be corrected, so that on average the thermal brightness is lower by about a factor of 2, and the cold brightness is on average higher, also by about a factor 2, with respect to the official data. However, in this work we stick to the comparison with the official yellow book values.

information available from the existing design. A preliminary design of the flow-channels was performed [28] and used for the final brightness calculations.

To determine absolute uncertainties on the brightness values one must also consider the uncertainties related to the Monte Carlo calculations. MCNPX calculations are based on spallation/evaporation models, and on nuclear libraries (available mostly up to 150 MeV energy), which includes also the scattering kernels. A detailed study of uncertainties related to these contributions was done during the work for the TDR mdoerator [1]. On the basis of those results, and considering the more mature level of the present design, we expect an absolute uncertainty of 15% on the brightness calculated from the model.

7. Summary and Conclusions

The design of the ESS moderators presented here is the result of an extensive work that considered all the relevant aspects to maximize the flux at the sample of the instruments. This approach allowed the selection of an optimal, bright source (the moderators), while ensuring that all the aspects related to beam extraction configuration, bispectral extraction, and phase-space transport were taken into account.

The results from the research of the optimal moderator design for ESS has had a profound impact on the configuration of the facility. The main results of this work are summarized below.

1) **Brightness increase by using low-dimensional moderators**. The flat moderators adopted for ESS offer a clear brightness increase with respect to the original TDR design based on volume moderators: the cold brightness increases by more than a factor of 2.5 with respect to the original design for ESS.

2) **Use of a single moderator system**. It was realized at an early stage that a single flat moderator would be sufficient, as the difference in performance between a single low-dimensional moderator with (2×120°) openings, and two low-dimensional moderators with (2×60°) openings each, would be negligible. This finding opened the possibility, eventually adopted, of having an initial instrument suite viewing moderators only above the target, with clear advantages in terms of performance, engineering, operation and upgradeability.

3) **Moderator shape for optimal beam extraction**. The chosen butterfly moderator is the best solution we could find to deliver high brightness to all instruments since it maximizes both thermal and cold brightness for a large (2×120°) opening angle and improves the beam extraction.

4) **Upgrade possibilities**. The chosen configuration, where all initial instruments foreseen for ESS point to the top moderator, leaves open several attractive possibilities for future use at ESS. Despite having all the instruments in the initial suite viewing the top moderator, the beam extraction system of ESS is designed so that all of the 42 beamports can view either the top or the bottom moderator, or even both.

With a high-brightness moderator at the top, the bottom area could be reserved in future for a source of neutrons which should be complementary to the top one. Several possibilities could be explored, such as:

Figure 31. Projected width at the thermal and cold moderator surface for the different beamports, for the butterfly 1 moderator. See explanation in the text.

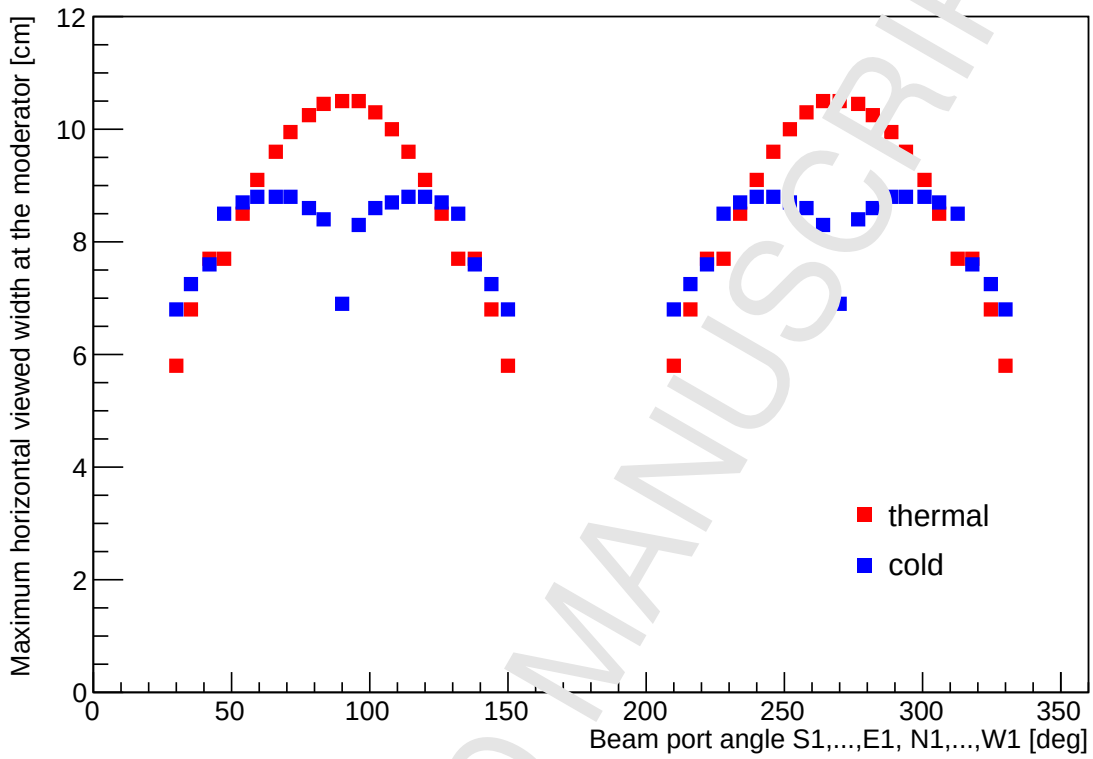

- Very Cold Neutron (VCN) source. There is increasing interest in VCNs for neutron scattering and fundamental physics applications [22]. The production of neutrons with $\lambda > 20$ Å requires different materials and temperatures than for cold neutrons. An interesting technique to increase the flux in this wavelength region might come by the use of diamond nanoparticle reflectors [31].

- High-intensity moderator, such as a large D_2 moderator, for specific experiments like the nnbar beamline [32, 33].

- A high-brightness moderator, even surpassing the brightness of the top moderator, which could be achieved either by using tube moderators (good for a few beam lines only, due to their strong directionality), or by further reducing the height with respect to the top moderator. Tube moderators are discussed in Appendix B.

Figure 32. Brightness distribution along a horizontal X axis perpendicular to the beamport direction shown for W1 and W11 beamports. Dashed lines pass through the focal points and the 0 of the X axis. At 90° (W11) the cold distributions from the two sides of the cold moderator have the same intensity, as expected.

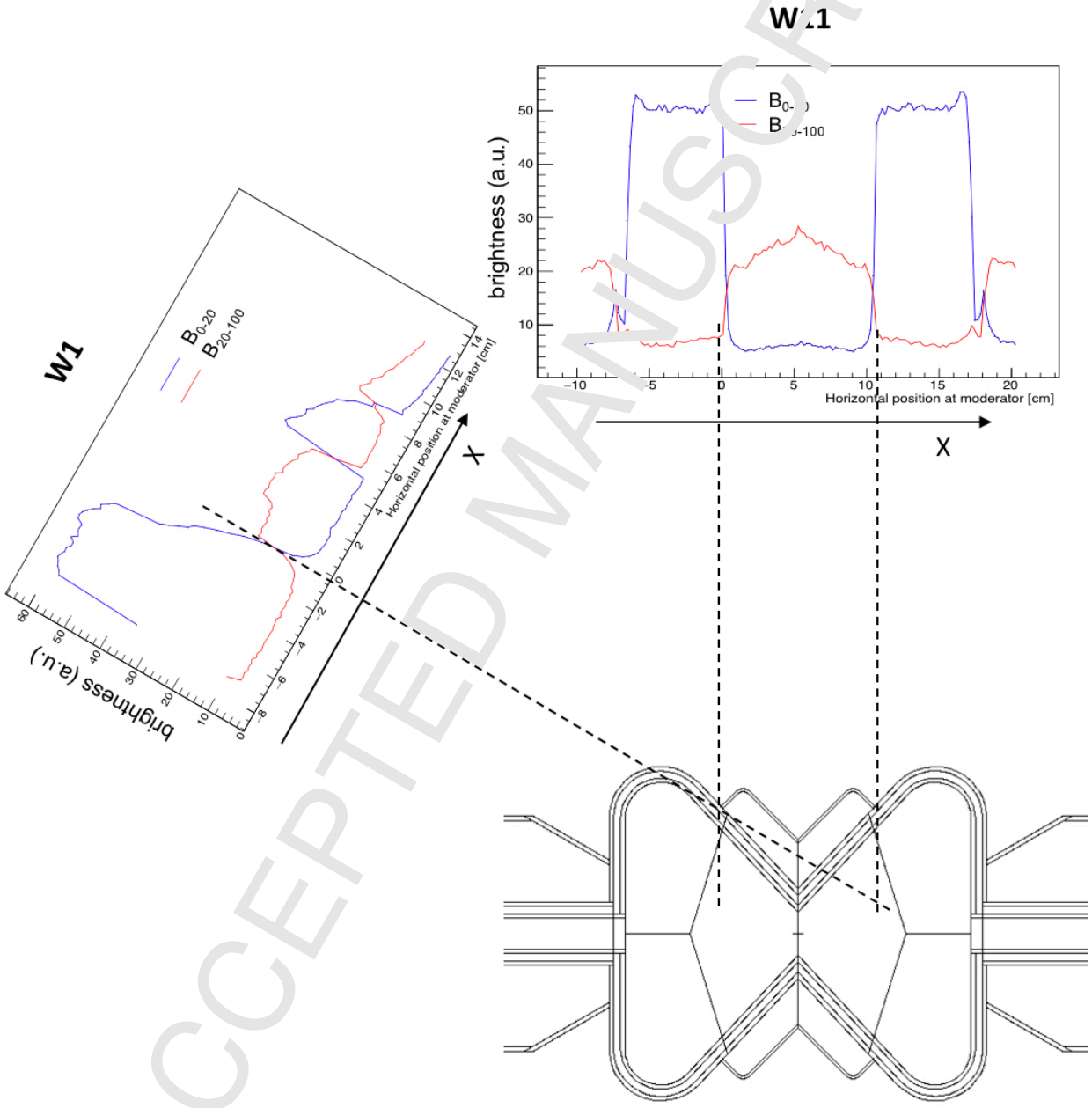

Figure 33. Horizontal brightness B_{0-20} and B_{20-100} distribution for the W3 beamport. The X axis corresponds to a line perpendicular to the beamport axis, with the 0 corresponding to the focal point (see Figure 32). These distributions are also valid for the S3, E3 and N3 beamports.

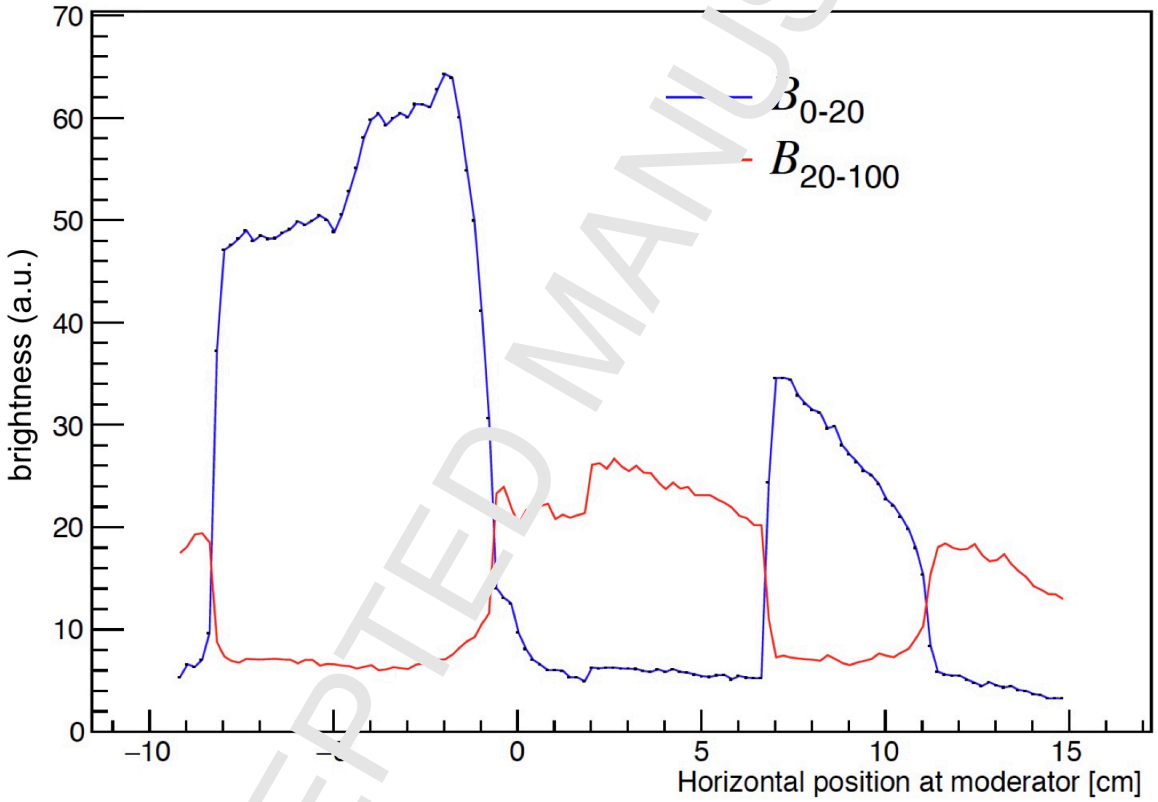

Figure 34. Distribution of B_{0-20} and B_{20-100} for the 42 beamports for the butterfly moderator with full engineering details.

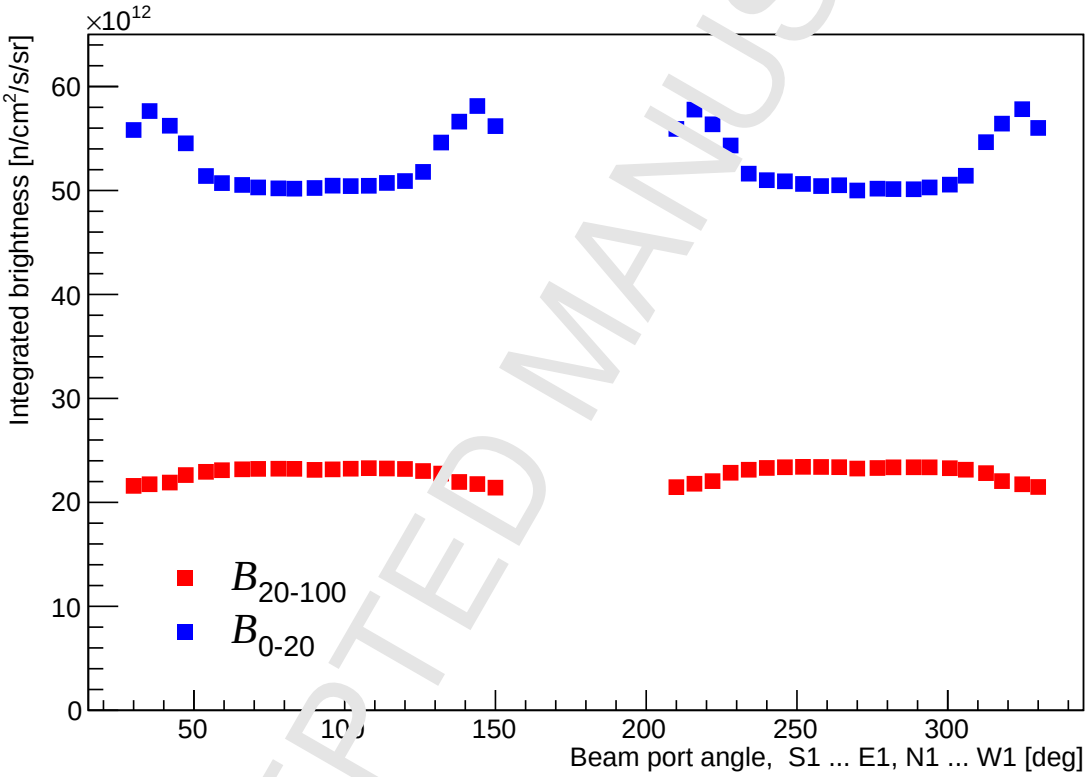

Figure 35. Thermal and cold peak wavelength spectral brightness. Spectra are averaged over the viewed moderator surface area of 3×6 cm^2.

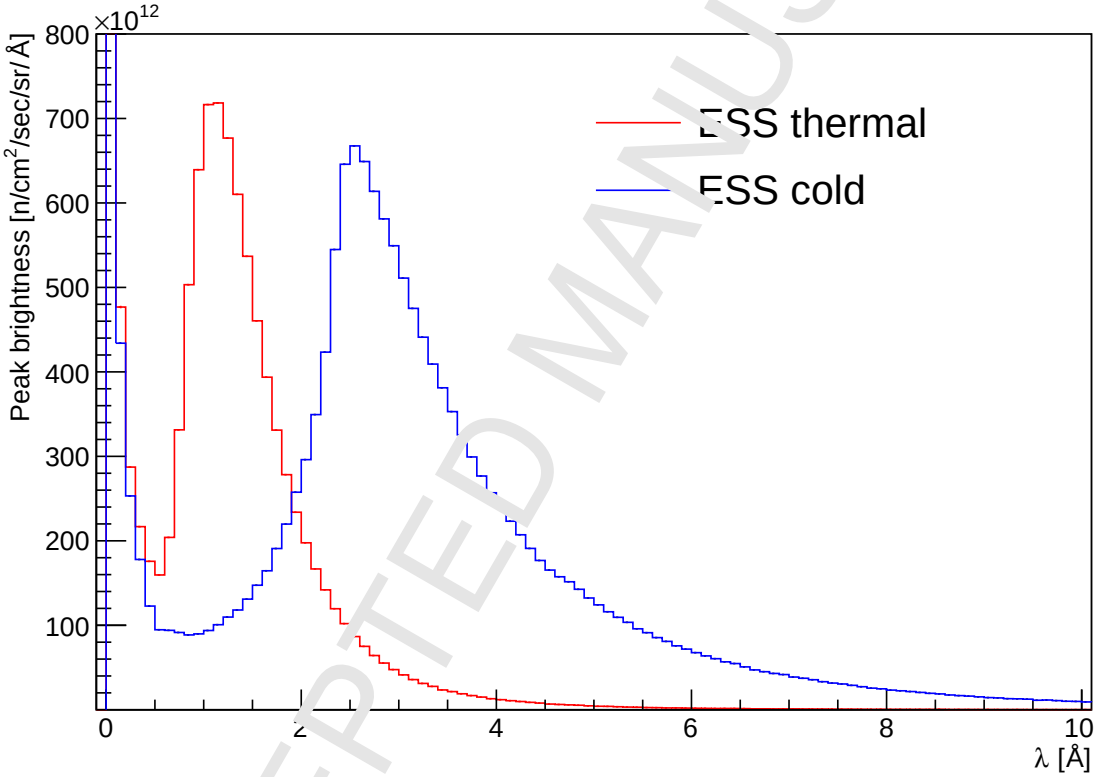

Figure 36. Brightness spectra averaged over 42 beamports for 3 cm high moderator, compared with ILL official curves [4].

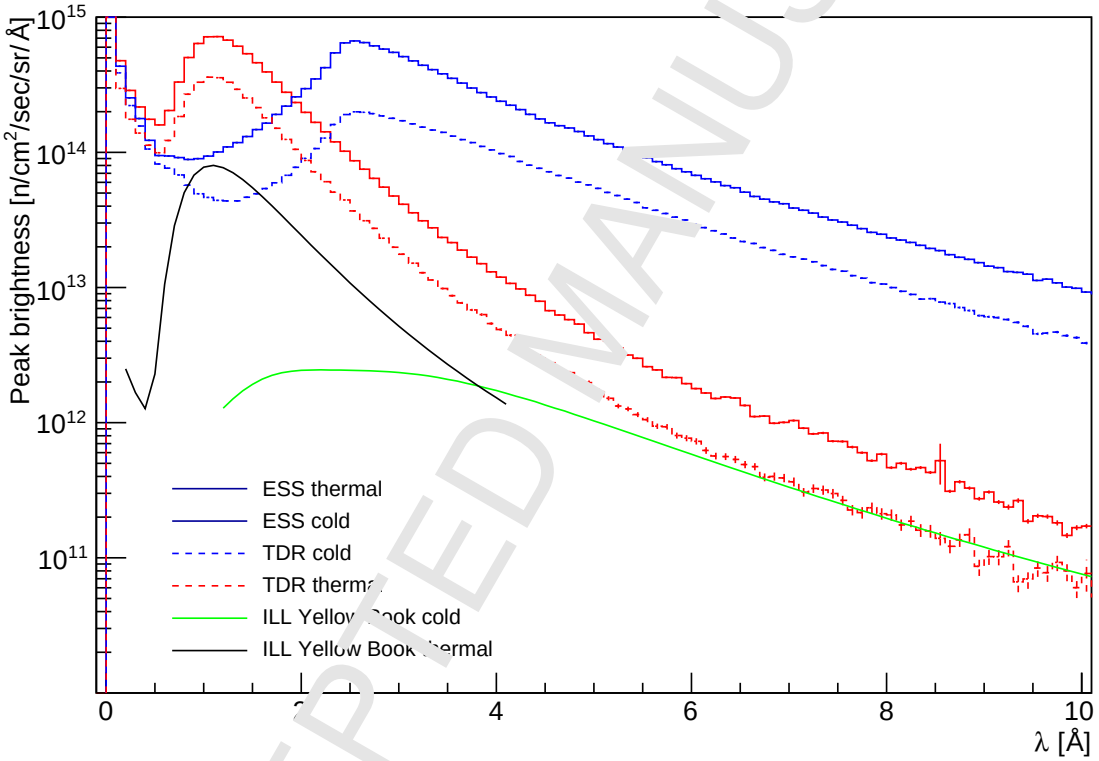

Figure 37. Cold collimators used in the MCNPX model for the brightness calculation. In the figure the collimators for the S1, S5 and S10 beamports are shown. The viewed width at the moderator is of 6 cm, the height is of 3 cm. The collimators intersect the point shown with the yellow dot, which is placed at 1.1 cm from the focal point (red dot), the origin of the axes of the beamports.

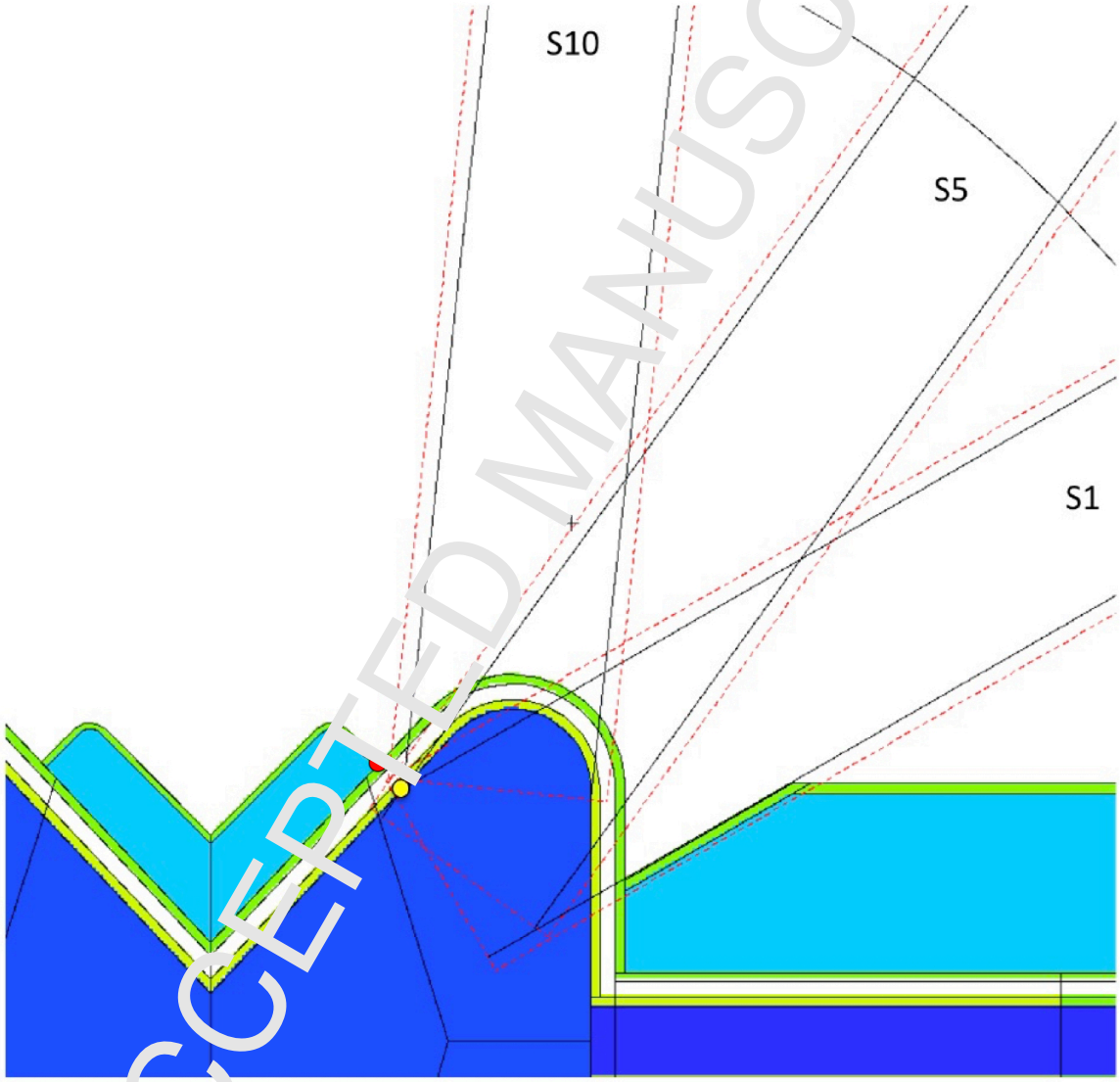

Figure 38. Geometry of box moderator.

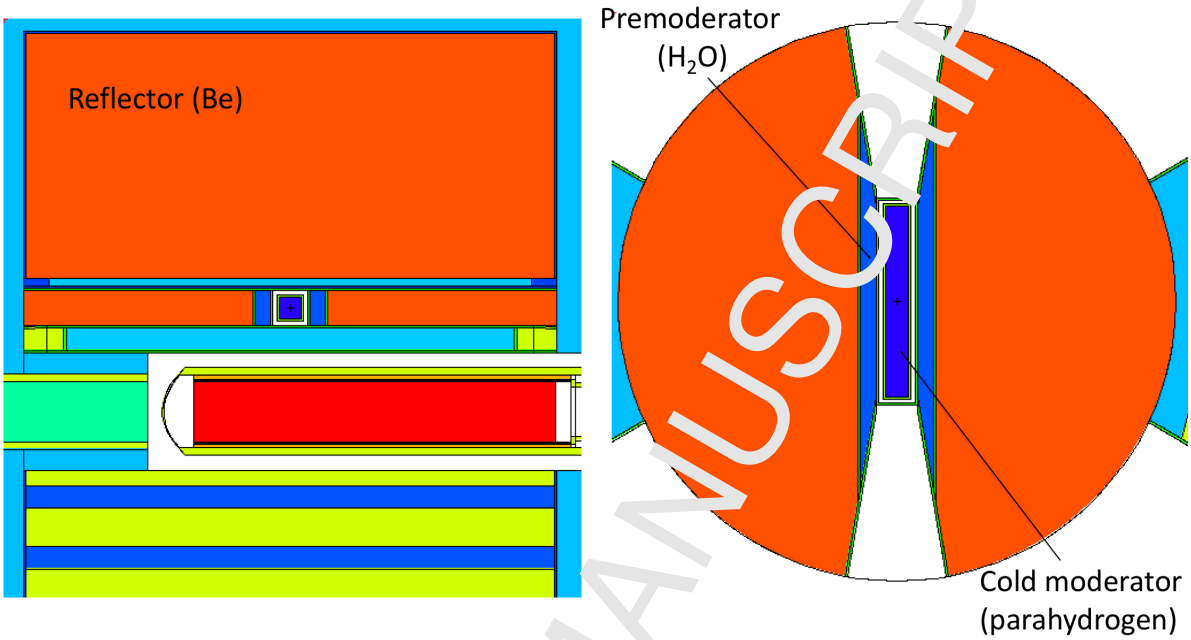

Figure 39. Brightness map as a function of lateral dimensions of a box moderator of 24 cm length.

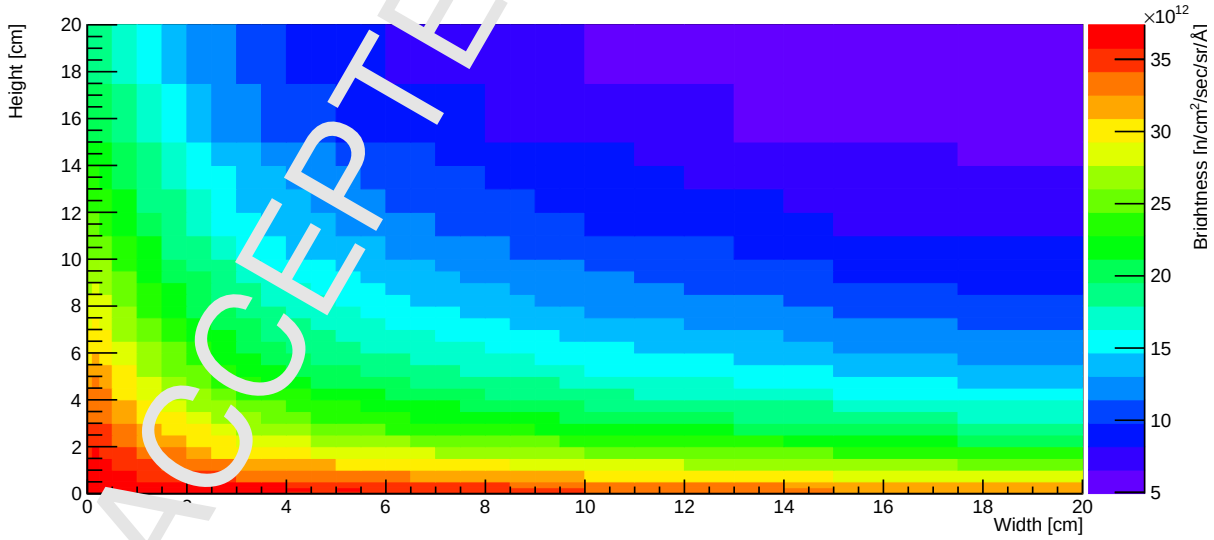

AppendixA. Brightness and figure of merit

AppendixA.1. Brightness and Liouville's theorem

We first show the link between the brightness of a source and Liouville's theorem, and, as a consequence, the fact that brightness is a constant of motion.

We define as neutron angular density $N(\mathbf{r}, \mathbf{\Omega}, E, t)$ the number of neutrons at the position $\mathbf{r}$ with direction Ω and energy E at time t, per unit volume, per unit solid angle, per unit energy. The vector position $\mathbf{r}$ can be at the surface of a moderator, while Ω is the direction of neutron emission:

$$N(\mathbf{r}, \mathbf{\Omega}, E, t) = \frac{n(\mathbf{r}, \mathbf{\Omega}, E, t)}{dV d\Omega dE} \tag{A.1}$$

The unit of N is n/cm^3/sr/eV.

The brightness B is the product of the speed v, times the neutron angular density.

$$B(\mathbf{r}, \mathbf{\Omega}, E, t) = vN(\mathbf{r}, \mathbf{\Omega}, E, t) = v\frac{n(\mathbf{r}, \mathbf{\Omega}, E, t)}{dV d\Omega dE} \tag{A.2}$$

The units of the brightness is n/cm^2/s/sr/eV.

On the other hand, the phase space density $\rho(\mathbf{q}, \mathbf{p}, t)$ is the number of particles in the phase space volume $d\mathbf{q}d\mathbf{p} = dVp^2dpd\Omega$ at time t:

$$\rho(\mathbf{q}, \mathbf{p}, t) = \frac{n(\mathbf{r}, \mathbf{\Omega}, E, t)}{dVp^2dpd\Omega} = \frac{v}{p^2}\frac{n(\mathbf{r}, \mathbf{\Omega}, E, t)}{dV d\Omega dE} \tag{A.3}$$

where we used the relationship between kinetic energy and momentum $E = \frac{p^2}{2m}$.

Liouville's theorem states that the phase space density $\rho(\mathbf{q}, \mathbf{p}, t)$, i.e. the number of particles in the phase space volume $d\mathbf{p}d\mathbf{q}$ at a given time t is constant along particle trajectories in phase space, for conservative force fields.

From the above two equations it follows that, for constant momentum, the neutron angular density and the brightness B are constant along the direction of motion.

These results are also valid if brightness is expressed as a function of the λ, as it is commonly expressed, instead of E.

In practical terms, conservation of the phase space density along the neutron trajectory (in phase space) means that knowing the brightness, it is possible to determine the absolute flux at any point of the beam extraction system. In reality, beam losses must also be considered. Neutrons emitted in a volume dV in direction $d\Omega$ around Ω will be transported in a guide system, assuming only elastic scattering collisions (with no change in neutron speed) and as the phase space density is constant, the divergence of the neutrons at the sample will depend on how focused is the beam (the more focused is the beam, the higher its divergence).

AppendixA.2. Figure of merit

To calculate the brightness with MCNPX we use f5 point detector tallies that calculate the flux at a point [8]:

$$\Phi(\mathbf{r}) = \int dE \int dt \int d\Omega v N(\mathbf{r}, \mathbf{\Omega}, E, t) \tag{A.4}$$

Thus, the f5 calculation integrates the brightness over 4π sr. If the integration is done in a solid angle $\Delta\Omega$, defined from a point at a distance r much greater than the moderator dimensions, that subtends only the moderator emission surface, so that the solid angle is $\Delta\Omega = \Delta S/r^2$, then the brightness defined by MCNPX is

$$B(\mathbf{r}) = \frac{\Phi(\mathbf{r})}{\Delta\Omega} \tag{A.5}$$

In practice, B can be calculated with specified bins in energy and time, so that, for small solid angles, B is a function of $(\mathbf{r}, \mathbf{\Omega}, E, t)$.

In this work we have often used the time-average, energy-integrated brightness between two energy values E_1 and E_2 defined as

$$B_{E_1-E_2}(r, \Omega) = \int_{E_1}^{E_2} dE \int_0^{\infty} dt B(\mathbf{r}, \Omega, E, t) \tag{A.6}$$

AppendixA.3. Tallies

Brightness is calculated for all the beamports in the two 120° beam extraction openings surrounding the moderators, using point detector tallies placed at 10 m from the moderator surface. The tallies are placed at the 42 angles corresponding to the actual beamport grid.

AppendixA.4. Collimators

The collimators are cells defined in MCNPX so that a point detector tally sees only the desired surface of the moderator (usually 6 cm wide, 3 cm high).

Figure 37 shows the viewed horizontal widths at the cold moderator used in the MCNPX model for brightness calculations. The viewed widths are defined by the solid lines, for all the beamports (in the figure as examples the beamports S1, S5 and S10 are shown). In all the calculations the vertical range seen at the moderator surface is always of 3 cm, while the reference horizontal width was of 6 cm. Due to the constraints from the beam extraction system discussed in Section 4, there is limited margin in the positioning of the collimators. A distance of about 1 cm from the focal point is allowed, and in the calculations the collimators were at 1.1 cm from the focal point (see Figure 37).

AppendixB. Tube moderators

Based on fundamental physics properties discussed in Section 2.1, the natural extension of quasi-2-dimensional flat moderators are quasi-1-dimensional "tube-like" moderators. A physics model of a tube moderator adapted to the ESS target-moderator-reflector layout is shown in Figure 38. To study the performance of such moderators we consider for convenience a box shape. This is a basic design which features a box-shaped parahydrogen moderator, surrounded by a premoderator and beryllium reflector. The geometry of the target and reflector is the same as in the other studies, allowing a direct comparison of the brightness. After an optimization of the premoderator thickness, the optimal length of a reference moderator with 3×3 cm^2 cross section was determined to be of 24 cm.

Then, with a fixed length of 24 cm, a two-dimensional brightness map as a function of width and height, size of emission surface given by (height × width), was calculated (Figure 39). The brightness map indicates a strong increase in brightness with decrease in the moderator height, as it has been already observed for the flat moderators. Increase in brightness with decrease in the moderator width is less pronounced. This is due to the size of the neutron production hotspot (cf. Figure 21). The immediate conclusion is that tube moderators would be particularly suitable for compact neutron sources where the size of neutron production region is comparatively small.

The stand-alone tube moderator of $3 \times 3 \times 24$ cm^3 exhibits cold B_{0-5} brightness about 2 times higher than the flat butterfly moderator. However, the tube moderator is highly directional and it can serve narrow extraction angles only. One way to increase the extraction angles would be to combine several tubes in different configurations.

Other examples of tube-like moderators, applied to small sources, are given in [34].

[1] S. Peggs editor, ESS Technical Design Report, ISBN 978-91-980173-2-8, 2013, http://europeanspallationsource.se/scientific-technical-documentation

[2] F. Mezei, *Long pulse spallation sources*, Physica B 234-236 (1997) 1227.

[3] M. Magán et al., *Neutronic analysis of the bispectral moderator such as that proposed for ESS*, Nucl. Instrum. Methods A729 (2013) 417425.

[4] Institut Laue-Langevin. 'ILL Yellow Book 2008.' http://www.ill.eu/?id=1379 , 2008.

[5] K. Batkov, A. Takibayev, L. Zanini and F. Mezei, Unperturbed moderator brightness in pulsed neutron sources, Nuclear Instruments and Methods in Physics Research Section A: Accelerators, Spectrometers, Detectors and Associated Equipment 729 (2013) 500 - 505. doi:http://dx.doi.org/10.1016/j.nima.2013.07.031.

[6] F. Mezei, L. Zanini, A. Takibayev, K. Batkov, E. Klinkby, E. Pitcher, and T. Schönfeldt, *Low dimensional neutron moderators for enhanced source brightness*, Journal of Neutron Research 17 (2014) 101 - 105.

[7] Waters L. S.*et al.* 2007 The MCNPX Monte Carlo radiation transport code. *AIP Conf.Proc.* **896**, 81-90.

[8] MCNP, *A general Monte Carlo N-Particle Transport code*, LA-UR-03-1987, 2003.

[9] D. Pelowitz editor, *MCNPX Users Manual, Version 2.7.0*, Number LA-CP-11-0438, 2011.

[10] L. Zanini, K. Batkov, E. Klinkby, F. Mezei, E. Pitcher, T. Schönfeldt, A. Takibayev *Moderator Configuration Options for ESS*, proceedings of the ICANS-XXI conference, JAEA-Conf 20-15-002, 2014.

[11] F. X. Gallmeier, W. Lu, B. W. Riemer, J. K. Zhao, K. W. Herwig, and J. L. Robertson, Conceptual moderator studies for the Spallation Neutron Source short-pulse second target station, Review of Scientific Instruments 87, 063304 (2016).

[12] U. Rücker, T. Cronert, J. Voigt *et al.*, Eur. Phys. J. Plus (2016) 131: 19. https://doi.org/10.1140/epjp/i2016-16019-5.

[13] K. H. Andersen, M. Bertelsen, L. Zanini, E. B. Klinkby, T. Schönfeldt, P. M. Bentley and J. Saroun, *Optimisation of moderators and beam extraction at ESS*, JAC 51, 264 (2018).

[14] N. Watanabe, *Neutronics of pulsed spallation neutron source*, Rep. Prog. Phys. 66 (2003) 339–381, and references therein.

[15] K. B. Grammer et al., *Measurement of the Scattering Cross Section of Slow Neutrons in Liquid Parahydrogen from Neutron Transmission* Phys. Rev. **B** 91, 180301(R) (2015).

[16] J. Schwinger and E. Teller, *The Scattering of Neutrons by Ortho- and Parahydrogen*, Phys. Rev. 52, 286 (1937).

[17] P. Rock, *Chemical thermodynamics; principles and applications* (Macmillan 1969). ISBN 1-891389-32-7

[18] T. Kai, M. Harada, M. Teshigawara, N. Watanabe, Y. Ikeda, *Coupled hydrogen moderator optimisation with ortho/para hydrogen ratio,* Nuclear Instrum. Methods in Physics Research A 523, 308 (2004).

[19] M. Harada, M. Teshigawara, M. Ohi, E. Klinkby, L. Zanini, K. Batkov, K. Oikawa, Y. Toh, A. Kimura, Y. Ikeda, *Experimental validation of the brightness distribution on the surfaces of coupled and decoupled moderators composed of 99.8% parahydrogen at the J-PARC pulsed spallation neutron source*, Volume 903, p. 38, 2018.

[20] R. Golub, K. Bning, and H. Weber, *Ultra-Cold Neutrons at the SNQ Spallation Source*, TUM-E21/SNQ-UCN/81-4, 1981.

[21] E. Klinkby, K. Batkov, F. Mezei, E. Pitcher, T. Schönfeldt, A. Takibayev, and L. Zanini, *In-Pile ^{4}He Source for UCN Production at the ESS*, Adv. High Energy Phys., 2014, 2014, p. 241639, doi 10.1155/2014/241639

[22] Micklich B.J. and Carpenter J.M (editors), Proceedings of the workshop on Applications of a Very Cold Neutron Source, August 21-24, 2005, Argonne, Illinois, ANL-05/42, Argonne National Laboratory (2005).

[23] L. Zanini, K. Batkov, F. Mezei, A. Takibayev, E. Klinkby, T. Schönfeldt, *The neutron moderators at the European Spallation Source*, proceedings of the AccApp'15 conference http://accapp15.org/wp-content/data/index.html, 2015.

[24] T. Schönfeldt, *Advanced Neutron Moderators*, PhD thesis Technical University of Denmark, 2017.

[25] L. Zanini, K. Batkov, E. Klinkby, F. Mezei, T. Schönfeldt, and A. Takibayev, *The neutron moderators for the European Spallation Source*, Journal of Physics Conference Series 1021(1):012066, DOI: 10.1088/1742-6596/1021/1/012066, 2018.

[26] Carpenter, Loong, *Elements of slow neutron scattering*, 2016.

[27] R. Garoby et al., *The European Spallation Source Design*, Physica Scripta, Vol. 93, N. 1, 2017.

[28] Y.Bessler, private communication, 2018.

[29] P. Willendrup, E. Farhi and K. Lefmann, *McStas 1.7 a new version of the flexible Monte Carlo neutron scattering package*, Physica B, 350 (2004) E735.

[30] T. Kittelmann, E. Klinkby, F. B. Knudsen, P. Willendrup, X. X. Cai, and K. Kanaki, Kalliopi, *Monte Carlo Particle Lists: MCPL*, Comput. Phys. Commun., 218, 17, 2017, ARXIV:1609.02792.

[31] V.V. Nesvizhevsky, E.V. Lychagin, A.Yu. Muzychka, A.V. Strelkov, G. Pignol, K.V. Protasov, *The reflection of very cold neutrons from diamond powder nanoparticles* Nuclear Instrum. Methods Physics Research A 595 (2008) 631.

[32] E. B. Klinkby, K. Batkov, F. Mezei, T. Schönfeldt, A. Takibayev, L. Zanini, *Voluminous D2 source for intense cold neutron beam production at the ESS*, in: arXiv physics eprints, No. arXiv:1401.6003, 2014.

[33] D. Milstead, *A new high sensitivity search for neutron-antineutron oscillations at the ESS*, arXiv:1510.01569v1

[34] L. Zanini, F. Mezei, K. Batkov, E. Klinkby and A. Takibayev, *General use of low-dimensional moderators in neutron sources*, Journal of Physics Conference Series 1021(1):012009, DOI: 10.1088/1742-6596/1021/1/012009, 2018

Table 1. Variation of the beamport-averaged brightness B_{0-20} on the top moderator as a function of different moderator or fast neutron reflector configurations below the target.

configuration	gain factor
two moderators	1
Be 10% water	1.09
Pb	1.20
W 22% He	1.18
Steel 10% water	1.10
Steel 20% water	1.07
Cu 20% water	1.09

Table 2. Time-average integral thermal and cold brightness in [n/cm^2/sr/s] for 5 MW average beam power of different moderator concepts. ESS peak brightness are 25 times the indicated numbers. In the last column the ILL Yellow Book brightness is listed [4].

	TDR	PC near	PC far	BF1	BF2	ILL YB
opening	$4 \times 60°$	$2 \times 120°$	$2 \times 120°$	$2 \times 120°$	$2 \times 120°$	
B_{20-100}	1.06×10^{13}	1.63×10^{13}	2.21×10^{13}	2.47×10^{13}	2.60×10^{13}	6.7×10^{13}
B_{0-20}	1.98×10^{13}	5.23×10^{13}	4.83×10^{13}	5.45×10^{13}	4.94×10^{13}	7.5×10^{12}